PERFORMANCE ANALYSIS OF KU BAND DVB-S2 VSAT SYSTEM

UNDER DUST AND SAND STORMS

BY

ABDULAZIZ MOHAMMED ALYAMI

A Thesis Presented to the

DEANSHIP OF GRADUATE STUDIES

KING FAHD UNIVERSITY OF PETROLEUM & MINERALS

DHAHRAN, SAUDI ARABIA

In Partial Fulfillment of the
Requirements for the Degree of

MASTER OF SCIENCE

In

TELECOMMUNICATION ENGINEERING

MAY 2014

KING FAHD UNIVERSITY OF PETROLEUM & MINERALS

DHAHRAN- 31261, SAUDI ARABIA

DEANSHIP OF GRADUATE STUDIES

This thesis, written by **Abdulaziz Mohammed Al-Yami** under the direction his thesis advisor and approved by his thesis committee, has been presented and accepted by the Dean of Graduate Studies, in partial fulfillment of the requirements for the degree of **MASTER OF SCIENCE IN TELECOMMUNICATION ENGINEERING.**

Dr. Samir H. Abdul-Jauwad
(Advisor)

Dr. Ali Ahmad Al-Shaikhi
Department Chairman

Dr. Kamal M. Harb
(Co-Advisor)

Dr. Salam A. Zummo
Dean of Graduate Studies

Dr. Ali Ahmad Al-Shaikhi
(Member)

9\7\14
Date

Dr. Sheikh Sharif Iqbal
(Member)

Dr. Samir Al-Ghadhban
(Member)

To My Parents

&

To My Advisors

ACKNOWLEDGMENTS

TABLE OF CONTENTS

LIST OF TABLES

LIST OF FIGURES

LIST OF ABBREVIATIONS

8PSK	:	8 Phase Shift Keying
ACM	:	Adaptive Code and Modulation
AAS	:	Adaptive Antenna Sizing
ACSTS	:	Advanced Communications Technology Satellite
BER	:	Bit Error Rate
BPSK	:	Binary Phase Shift Keying
BS	:	Broadcasting Satellite
C Band	:	IEEE C-band (4 GHz to 8 GHz)
CCM	:	Constant Code and Modulation
CDMA	:	Code Division Multiple Access
DBS	:	Direct Broadcast Satellite
DTH	:	Direct to Home
DUSA	:	Dust and Sand Attenuation
DVB	:	Digital Video Broadcast
DVB-RCS	:	Digital Video Broadcast – Return Channel via Satellite
DVB-S1	:	Digital Video Broadcast - First Generation
DVB-S2	:	Digital Video Broadcast - Second Generation
ETSI	:	European Telecommunications Standards Institute
FEC	:	Forward Error Correction
FSK	:	Frequency Shift Keying
FSS	:	Fixed Satellite Service
GPS	:	Global Positioning System
GSM	:	Global System for Mobile
GTRI	:	Georgia Technology Research Institute

HDTV	:	High Definition Television
HTS	:	High Throughput Satellite
IDU	:	Indoor Unit
IPTV	:	Internet Protocol Television
ITU-R	:	International Telecommunications Union – Radiocommunication
Ka Band	:	K-above / IEEE Ka-band (26.5 GHz to 40 GHz)
Ku Band	:	K-under / IEEE Ku-band (12 GHz to 18 GHz)
LNB	:	Low Noise-Block Downconverter
LPDC	:	Low Parity Density Coding
LTE	:	Long Term Evolution
MBA	:	Multi Beam Satellite Antenna
MF TDMA	:	Multi Frequency Time Division Multiple Access
MSK	:	Minimum Shift Keying
NASA	:	National Aeronautics and Space Administration
NSR	:	Northern Sky Research
ODU	:	Outdoor Unit
OQPSK	:	Offset Quadrature Phase Shift Keying
PAM	:	Pulse Amplitude Modulation
QAM	:	Quadrature Amplitude Modulation
QoS	:	Quality of Service
QPSK	:	Quadrature Phase Shift Keying
RF	:	Radio Frequency
SNR	:	Signal to Nosie Ratio
TRF	:	Traffic (burst type)
VCM	:	Variable Code and Modulation
VSAT	:	Very Small Aperture Terminal

THESIS ABSTRACT (English)

Full Name: ABDULAZIZ MOHAMMED NUQTAN ALYAMI

Thesis Title: PERFORMANCE ANALYSIS OF KU BAND DVB-S2 VSAT
                              SYSTEM UNDER DUST AND SAND STORMS

Major Field: TELECOMMUNICATIONS ENGINEERING

Date of Degree: MAY 2014

Now a days, the industry's need for Ku-band satellites is in increase due to the capacity abundance and cost efficiency. The commonly used C-band satellites have limited number of geosynchronous orbital slots for given frequency band, thus industries are turning to Ku-band satellites. These Ku-band satellites operate in higher frequencies (12-18 GHz) making them vulnerable to atmospheric conditions like rain, temperature, dust, humidity, etc. The weather conditions are usually rough in Saudi Arabia. The area mainly consists of deserts and the temperature is usually high. There are also frequent dust and sand storms that attenuates the Ku-band signals. This thesis proposes a dust and sand storms attenuation (DUSA) model based on physical measurement and compares it with readily available models in the literature. Also, this thesis work proposes some techniques that mitigate the environmental effects of dust and sand storm to ensure improved data rates and quality of service (QoS) for Very Small Aperture Terminal (VSAT) systems. In order to get accurate results, simulations are carried out using the metrological parameters values of physical instruments. These results are then analyzed in DVB-S2 VSAT system in which a controller is proposed that will measure the effect and adjust the channel parameters for better throughput during different weather conditions.

ملخص الرسالة

الاسم الكامل: عبدالعزيز محمد نقطان آل بحري اليامي

عنوان الرسالة: تحليل أداء نظام KU BAND VSAT تحت تأثير العواصف الرملية و الترابية

التخصص: هندسة اتصالات

تاريخ الدرجة العلمية: مايو 2014

في هذا الوقت، حاجة الصناعات للأقمار الصناعية ذات نطاق تردد Ku في تزايد بسبب وفرة القدرات و كفاءة التكلفة. يشيع استخدام الأقمار الصناعية التي تعمل على نطاق تردد C اللتي لديها عدد محدود من فتحات المدار المتزامن مع الأرض. وبالتالي، الصناعات قائمة على تحويل إتصالاتها الى الأقمار الصناعية ذات نطاق تردد Ku. هذه الأقمار تعمل على ترددات عالية (12- 18 غيغاهرتز) مما يجعلها عرضة للظروف الجوية مثل المطر ودرجة الحرارة والغبار و الرطوبة، وما إلى ذلك من الظروف المناخية وعادة ما تكون قاسية في المملكة العربية السعودية والتي تتكون أساساً من الصحاري و درجة الحرارة عادة ما تكون مرتفعة. هناك أيضاً كثرة الرمال و العواصف الترابية التي تضعف من قوة إشارات نطاق تردد Ku. تقترح هذه الأطروحة نموذج لتوهين العواصف الرملية والترابية لإشارات نطاق تردد Ku مبنياً على قياسات طبيعية و من ثم مقارنة هذا النموذج مع النماذج المقترحة من قبل باحثين آخرين. أيضاً، يقترح هذا العمل بعض التقنيات التي تخفف من الآثار البيئية للعواصف الرملية و الترابية لضمان تحسين معدلات البيانات وجودة الخدمة (QoS) لأنظمة VSAT. من أجل الحصول على نتائج دقيقة، تتم المحاكاة باستخدام قيم العوامل المناخية باستخدام الأدوات المناسبة. ثم يتم تحليل هذه النتائج في نظام VSAT DVB-S2 الذي يقترح وحدة تحكم من شأنها قياس تأثير و ضبط العوامل المؤثرة لتحسين الإنتاجية أثناء ظروف الطقس المختلفة.

CHAPTER 1

INTRODUCTION

Wireless communications cover the frequency spectrum starting at 3 *Hz* and ending at 300 *GHz*. A brief review of frequency spectrum is shown in Figure 1.1. The commonly used bands for satellite communications are shown in Figure 1.2. Each of these bands has its advantages and limitations. Practically, normal broadcasting is not done at low-end frequencies so these are of little interest from satellite communication aspect. Low frequencies require a large antenna and a very high transmit power so these are not used for satellite communications. However, these ranges may be used for underwater communication in submarines and underground communication in mines or some geophysics measurements. The major drawback of using low frequencies is that high data rate is not possible via signals of low frequencies.

The appropriate range for satellite communication is shown in green bar of Figure 1.1 which is ranging from 20 *MHz* to 40 *GHz*. This range is suitable as signals are not significantly attenuated in by earth atmosphere and may be considered for satellite communications purposes. Figure 1.2 highlights the different high frequency bands used in satellite communications which shows that the Ku band's frequency space (6 *GHz* from 12 to 18 *GHz*) is much greater than the C band currently in use. Ku band is primarily used for fixed and broadcast satellites. Ku band ranges from 12 *GHz* to 18 *GHz* and it is divided into segments. Each segment is allocated to different regions of the world for communications. Earlier, C band was the only used band for satellite communications. However, the number of satellites is growing rapidly and the need for global broadcast and communications proved its

importance. The need for high data rates with very less delay has been raised across the globe. In order to cater the increasing needs of data for local and commercial customers, new satellites with improved technologies are built. Spectrum is a scarce resource and C band could accommodate a very little number of satellite links. Hence, Ku band is now serving the increasing demands of satellite communications. Small and cheap antennas were only possible due to usage of Ku bands in which many home satellite solutions are now possible due to small antenna sizes.
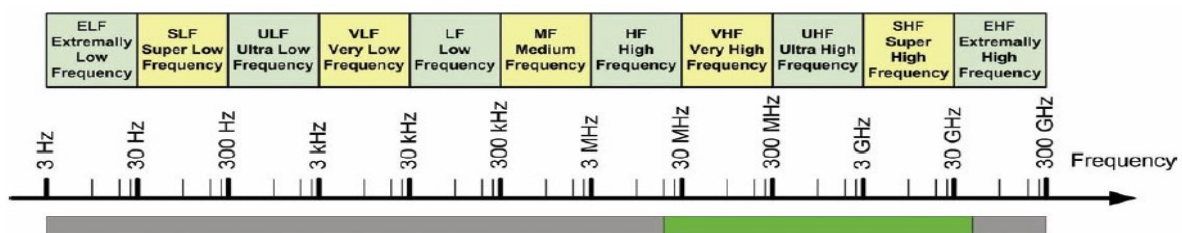
Figure 1.1: Frequency spectrum [1].
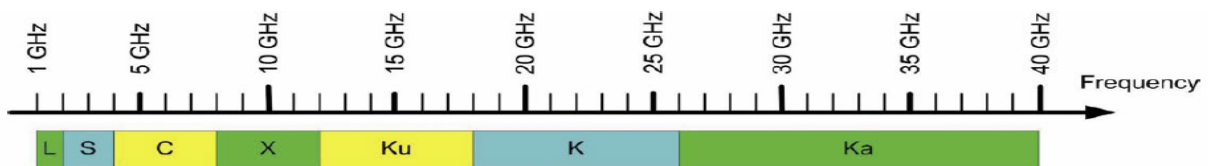
Figure 1.2: Satellite communications bands [1].

1.1   High Frequency Bands usage by Satellite Networks

The satellite service providers are targeting the consumer market for the provision of broadband access, knowledge of information, communication technologies and other multimedia applications [1]. The availability of alternative services such as DSL or cable is not common in rural and sub-urban areas as cable network requires a large infrastructure to be deployed before service. Since the 80's, constant development and research are being put

2

into the field of satellite communications and as a result deployed infrastructure is reducing with advancement. Higher data rates are now achievable in small satellites. Currently, deployed satellites could carry voice and data from one point to another with minimum delay and loss. High data rates can be provided to customers for industrial and home use in remote areas. Based on the type of system and technology, satellites could be divided into three generations [2].

1.1.1   First Generation Satellites

This generation was deployed in 1980s. The satellites have the following characteristics:

1   Supports data rates i.e. 56 *kbps* – 256 *kbps* per user.

2   Supports proprietary non IP based protocols were used for communications.

3   Characterized by bursty data usage with limited need of real time circuits.

4   (Very Small Aperture Terminal) VSAT terminal costs around US $5000 - $10,000.

1.1.2   Second Generation Satellites

This generation was deployed between 2005 – 2007 with the following characteristics:

1   Supports high data rates i.e. 256 *kbps* – 3 *Mbps* per user.

2   Supports IP routing technology and QoS is used.

3   Uses Software defined modems with advanced modulations schemes.

4   VSAT terminal cost reduced to US $500.

5   Handles real time data extending support for voice services.

1.1.3   Third Generation Satellites

These VSATs were deployed from 2010 onwards to cater the upcoming demands of high data rates of users. These satellites support:

1   Throughput greater than 12 *Mbps* per user.

2   Video driven applications.

3   IP routing technology.

4   VSAT terminal cost reduced further less than US $500.

Detailed comparison can be seen in Figure 1.3

Characteristic	First Generation	Second Generation	Third Generation
Timeframe of Operation	1980s to present	mid 2005 to present	2010+
	Increasing Satellite Capacity →		
Satellite Capacity	1 Gbps	10 Gbps	100 Gbps
	Increasing Data Rate per User (Improved User Experience) →		
Typical Data Rate per Terminal	56 kbps - 256 kbps	256 kbps - 3 Mbps	2 Mbps - 30 Mbps
	Increasing Number of Subscribers →		
Maximum Number of Subscribers per Satellite	100,000 - 500,000	750,000 - 1,000,000	2 million - 3 million
Satellites	All FSS satellites; Example: Hughes leases 126 xpnders worldwide	IPStar; SES ASTRA2Connect; Eutelsat TooWay; Wildblue; Telesat; Spaceway	ViaSat-1; KA-SAT; KaComm; SpaceWay 4
Satellite Payload Characteristics	24 Ku-band transponders w/ regional coverage & 36 - 72 MHz bandwidth	Ku-band & Ka-band spot beams w/ 36 - 72 MHz bandwidth	Ka-band spot beams w/ ~500 MHz bandwidth
Major VSAT Terminal Suppliers	Hughes, Gilat, ViaSat, iDirect	Hughes, Gilat, ViaSat, iDirect	Hughes, Gilat, ViaSat, iDirect
Cost of VSAT Terminal	$5,000 - $10,000	$500 - $1,000	< $500
Typical Applications	Point-of-sale transactions	Broadband access for enterprise & consumer	Broadband access for enterprise & consumer
Data Protocol	Proprietary and non-IP based	IP based	IP based
Connection Type	Bursty; Non-real-time data	Continuous; VoIP & video streaming capable	Continuous; VoIP & video streaming capable

Figure 1.3: Comparison of satellite generations [3].

It is envisaged that the deployment of smaller and portable satellites will become ubiquitous in near future due to their rapid installation and easy operation. Indeed, consumers and businesses in rural and remote areas can be served with two-way broadband and high-speed Internet services at much cheaper cost via Ku band satellite communications technology.

There is a requirement to minimize the expected regulatory burden on Ku band satellite systems and to ensure the development of such satellite networks for broadband services by large-scale deployments of terminals. Many regulatory decisions have proven beneficial to the deployment of satellite systems in Ku band like licensing exemption in various ranges for earth stations. Satellite communications systems connect large numbers of users over large distances thus enabling telecommunication services over wide geographical areas. The satellites have become an important part of the telecommunications infrastructure because of low cost equipment and matured technology. Currently, we find numerous satellite services including VSAT networks, satellite broadband services, global Internet services using microwave links, point-to-point links, direct-to-home (DTH) receivers and mobile satellite service using feeder links. Satellites support critical governmental infrastructure like environmental alerts, water, weather and climate alerts, use for civil and military aviation and other governmental uses.

The electronics communication markets are growing most rapidly around the globe and have become the key element of the developments in the world. The increasing competition in this market is causing broadband prices to go down and speed to go up resulting into consumers benefiting from a wide variety of broadband offers on cheap rates. The operators are eager to get newer technologies due to commercial nature of the satellite market. Additionally, the developed nations have set themselves the goal of creating new job opportunities due to recent global recession and are providing a favorable environment for private investment.

This can enable everyone to participate in the global information society, modernizes public services and boosts productivity.

1.2   NASA's Advanced Communication Technology Satellite

Since early 60's, the national aeronautics and space administration (NASA) is developing the communications satellites ranging from the early passive repeaters to the modern rocketry and space exploration equipment. Early developments by the NASA were experimental due to the very little knowledge available about operating satellite communications systems. Nevertheless, over a period of time, the technology has matured and many private agencies, governments and individual groups had started developing and operating private satellites.

The advanced communications technology satellite (ACTS) was the first attempt by the US to use the Ku-band for satellite communications launched in 1993 which was NASA's program to maintain the U.S. prominence in the space, propagation measurements and reducing the risk of developing novel technologies that cannot be covered by private sector's sponsorships. The proposed usage incorporated beacons on the satellite to provide this opportunity. The ACTS incorporated various other technologies like multi-beam antennas, wideband microwave switch matrixes, baseband processor and adaptive compensation techniques due to rain fade [2]. Both the satellite and terrestrial services are required to seamlessly interconnect for which the technologies ACTS are providing are crucial for future's systems to be developed.

1.3   The Need for Ku Band Satellite Services

The future networks are required to possess following desirable characteristics:

1. Broadband - high data rate (in Gigabits per second) in all configurations of networks i.e. point to point or point to multi-point.
2. Narrowband - low data rate (in Kilobits per second) in networks used for personal communications using small or ultra-small aperture terminals.

The fixed service satellites (FSS) based on Ku band have high power and broad coverage and are highly optimized for video dissemination and data networks. There are various advantages associated with Ku band satellite broadband applications in comparison to other broadband solutions. Also, there are drawbacks with respect to their suitability depending on the environment considered which needs to be carefully considered. An important advantage of satellite Ku band is its usage to decrease digital divide in urban-rural areas to cover first-mile connectivity gaps in rural/ remote areas due to expensive fiber optical links.

The global congestion of available orbital locations and steady increase in the demand for satellite capacity has limited the traditional FSS satellite technology using Ku band frequencies. Importantly, the flexible distribution of bandwidth needed for broadband applications in today's world are not effectively supported by old systems built to cover a very large geographical area. The new technology of multiple-beam satellite antennas (MBA) allows frequency reuse and maximizes bandwidth capacity and has become a key component in modern broadband satellite communication systems. The use of Ku band frequencies in broadband satellites associated with multiple thin spot beams enables the MBA technology to be even more efficient. Moreover, the antenna technology has advanced causing antennas to be smaller in size and cheaper in price.

1.4   Saudi Aramco Collaboration

This work is done in cooperation with Saudi Aramco which is one of the leading oil and gas companies of the world. Major operations of this company include exploring, drilling, refining and distributing petroleum products all over the globe. This company operates in all regions of the world. There is a constant requirement of real time communications between site offices and regional offices. Since oil and gas explorations are majorly done in rural areas, so cable network is not feasible. To fulfill the communications needs, Saudi Aramco has its own VSAT network which supports data and voice communication network and reliability through redundant network links and elements. Like other industries, Saudi Aramco is also expanding and finding new opportunities. With new opportunities there comes the need for more resources. Since this company is based in Saudi Arabia which is known for dust, sand storms and extremely high temperatures so a controller is needed to be designed that can alter the communication parameters sensing the climate conditions. This will help in creating a link with higher data rates to its subsidiaries irrespective of weather. Saudi Aramco currently has latest DVB-S2 VSAT that supports point to multipoint communication, adaptive coding scheme.

1.5   Thesis Contributions

The focus in this thesis work is to evaluate the performance of a Ku band based DVB-S2 VSAT system under dust and sand storms, quantify their impact on satellite links by proposing a signal attenuation model, and suggest mitigation techniques to counteract their effects. Analysis and evaluation of satellite links performance using simulated channel considering the proposed attenuation model is performed. Signal to noise ratio (SNR), bit error rate (BER), and spectral efficiencies were analyzed. In particular, this work will have the following contributions:

(a) Conducting a comprehensive study of the weather variation for the area under investigation namely Dhahran, Saudi Arabia.

Description: The starting point of this thesis work is to study the different metrological parameters affecting the satellite communication links namely haze and contents of the air, visibility and air humidity.

(b) Formulating a methodology for estimating dust and sand attenuations based on latest techniques available in literature and incorporating metrological data obtained from physical measurements.

Description: Study the effects of dust and sand storms on Ku-Band DVB-S2 VSAT networks in the region of Saudi Arabia. Prediction of attenuation on satellite signals due to dust and sand storms is the sole objective of this milestone.

(c) Proposing a self-healing system that is adaptively updated utilizing back-propagation learning and artificial intelligence based algorithms.

Description: The input to such system is the estimated values of dust and sand storm metrological parameters. The output will be the modified parameters of VSAT system to enable end-to-end performance enhancement. The modified parameters include: adaptive antenna sizing (AAS), adaptive code and modulation (ACM), and uplink power control (UPC).

1.5.1   Thesis Related Publications:

The below publications are the outcomes during my thesis research period at KFUPM:

Published papers:

- Abdulaziz Al-Yami, Kamal Harb, B. Omair, Samir H. Abdul-Jauwad, and A. Al-Yami, "Analysis of Dust and Sand Storms Induced Impairments on VSAT Links in Saudi Arabia", International Conference on Computer, Control, Informatics and its Applications 2013 (IC3INA 2013), Indonesia, Nov. 2013.

- Kamal Harb, B. Omair, Samir H. Abdul-Jauwad, and Abdulaziz Al-Yami, "Systems Adaptation for Satellite Signal under Dust, Sand and Gaseous Attenuations", Journal of Wireless Networking and Communications, Vol. 3, No. 3, pp. 39-49, 2013.

- Kamal Harb, B. Omair, Abdulaziz Al-Yami, and Samir H. Abdul-Jauwad, "Probabilistic Dust Storm Layers Impacting Satellite Communications", Proc. of the IEEE International Conference on Space Science and Communication (IconSpace 2013), Malacca, Malaysia, pp. 407-411, July 2013.

- Kamal Harb, B. Omair, Samir H. Abdul-Jauwad, A. Al-Yami, and Abdulaiz Al-Yami, "A Proposed Method for Dust and Sand Storms Effect on Satellite Communication Networks", Innovations on Communication Theory (INCT 2012), Istanbul, Turkey, pp. 33-37, Oct. 2012.

Submitted papers:

- Abdulaziz Al-Yami , Kamal Harb, and Samir H. Abdul-Jauwad, "Performance Analysis of Ka Band VSAT System Under Dusty Weather Conditions", 7th Advanced Satellite Multimedia Systems Conference /13th Signal Processing for Space Communications Workshop 2014 (ASMS/SPSC 2014), Livorno, Italy, September 2014

1.6   Thesis Outline

Chapter 1 presents a general overview for the different satellite systems and emphasizes on the need of the Ku band satellites. Literature review is covered in Chapter 2. Chapter 3 discusses the different attenuation models for dust and sand storms on satellite communications channels in details and suggests methods to cater these attenuations. Chapter 4 presents verification results for different field measurements that estimate the attenuation due to dust and sand storms. In this chapter, multiple comparisons are summarized and evaluated. At the end of the chapter, multiple techniques to compensate for the induced attenuation in dust and sand storms on the satellite links are evaluated. Chapter 5 provides a summary, conclusions, and recommended future works.

CHAPTER 2

BACKGROUND AND LITERATURE REVIEW

2.1   Spectrum Requirements Forecasts

The future spectrum requirements will increase gradually in the next ten years independently from the method and assumptions used as indicated in Figure 2.1. This forecast made by northern sky research (NSR) is based on users in rural regions without a digital subscriber line (DSL) connection from 2008 onwards till 2018. It shows a decrease of subscribers on systems using regular load via C band versus multiple thin-spot beam payloads via Ku or Ka bands. The forecast in Figure 2.2 indicates a requirement of 323 Gigabits per second in year 2018 equivalent to bandwidth of about 120 *GHz* in Ka band. Ultimately, satellite industry would require even higher capacity after 2018 keeping this high growth rate in mind. It is expected that other applications will require even more However, investigations by NSR presented in Figure 2.1 indicate that the demand for high throughput satellites (HTS), the new generation of Ku-band satellites will be shown around 2013. The high throughput is possible because HTS typically implement 10 times wider transponders in the range of 300 *MHz* – 600 *MHz* compared to the standard Ku-band transponders in the range of 27 *MHz* to 54 *MHz* by making use of wider spectrum and multiple beams. As a consequence, the satellite operators are showing keen interest in Ku-band due to high capacity and possibility for better broadband services [2].
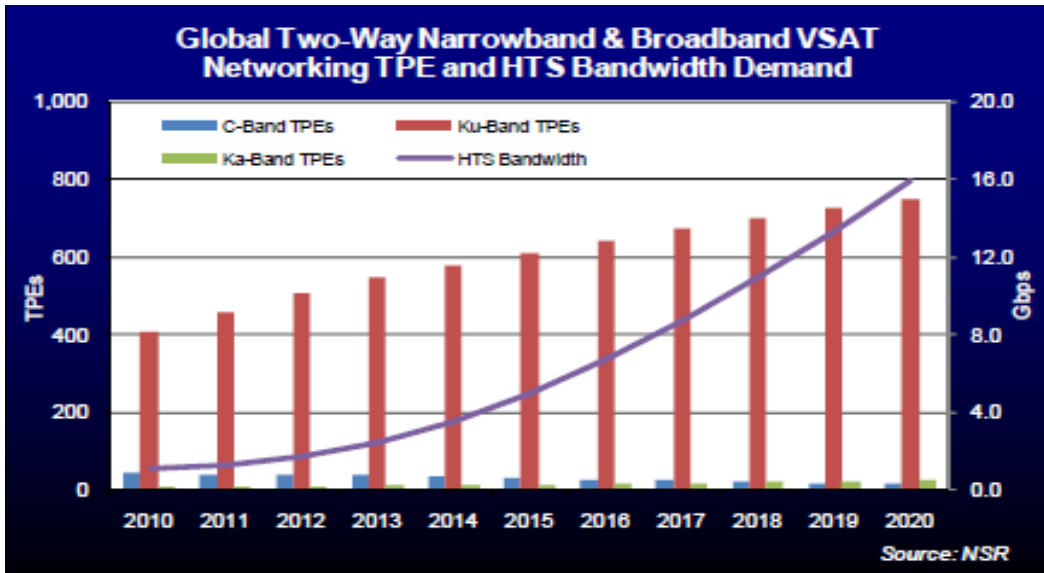
Figure 2.1: High throughput satellite and VSAT global transponder capacity demand [2].

The high throughput rates bring this technology at par with the state of the art today like 4G, long-term evolution (LTE) cellular and very high data rate services.
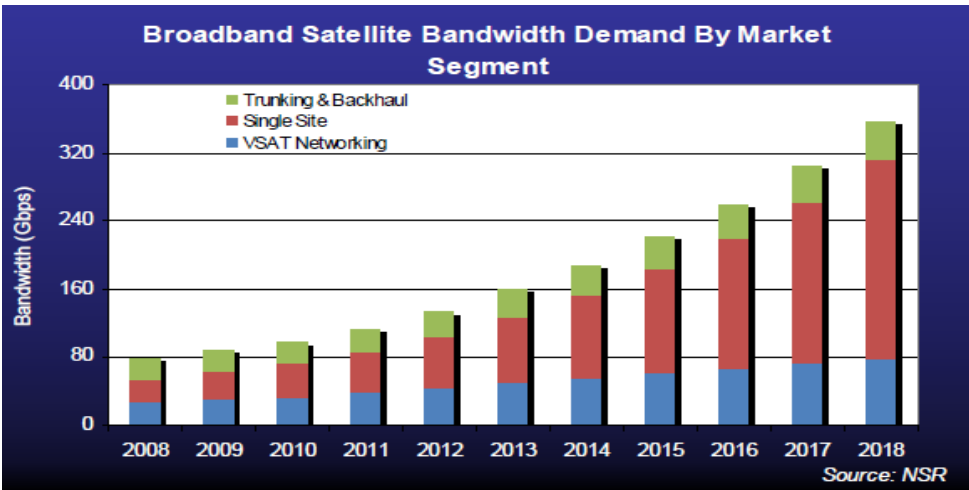
Figure 2.2: Worldwide broadband satellite bandwidth demand by market segment [2].

2.2 Ku Band Satellites

In contrast to C band satellites, Ku band satellites are not restricted in terms of power, hence, more immune from interfering with other wireless networks where the forward and return links powers can be increased.

Since the power can be adaptably increased, it indicates that the antennas can get smaller and smaller as the power increases. Antennas would be more capable when pointing them as frequency increases. An antenna with 1 *m* size operating at the Ku band can be pointing to one satellite and discarding signals coming from other satellites within 2 degrees at geostationary earth orbit (GEO). On the other hand, to attain similar performance, an antenna with 3 *m* size operating at the C band is required. The beam width of the antennas on both bands is becoming more crucial than the gain due to the fact that the power levels have increased for both bands. The Ku band provides resilient and cheap solutions to customers by enabling the production of low cost antennas and easing the processing of finding a proper place for the antennas installation.

Except for few provinces, the Kingdom of Saudi Arabia (KSA) is characterized by desert climate where dust and sand storm are commonplace due to large variations in temperatures at day and night. We find huge installations and heavy investment on high frequency wireless communication systems and networks throughout KSA due to various applications operating in these ranges. The performance degradation in service of such applications have been observed which include but not limited to mobile phones based on global system for mobile (GSM) and code division multiple access (CDMA) technologies, analog radios and radio station transceivers, digital pagers, high definition television systems, space based satellite navigational aids like global positioning system (GPS) and broadband services based on satellites. These systems make use of radio frequency (RF) and/or micro/millimeter wave

propagation near the ground in various line configurations. These waves attenuate heavily through absorption and energy scatter due to climate conditions like heavy clouds, foliage, rain, dust, and sand storms.

Due to the particular nature of weather in KSA, dust and/or sand storms greatly affect a large number of satellites as well as terrestrial links degrading their performance. Subsequently, many researchers have shown great amount of interest in studying the high frequency wave attenuation due to dust particles [2]-[15]. Electrical properties of climate conditions and the attenuation and phase shift due to scattering of dust and sand particles in the region of interest have been computed to quantify such effects. The complexities arise; as the computations require modeling when taking into account the contrasting factors like frequency, wavelength, size and shape of dust and sand particles, permittivity issues, concentration, visibility, moisture content in dust particles, and orientation relative to wave polarization.

Current satellite communication systems are based on Ku-band which incorporates a large number of commercial applications including many systems based on low margin VSATs. The atmospheric propagation degradations have great effects on the link availability and quality of transmission in such systems. This literature survey is aimed at evaluating the performance degradation in satellite communications systems specifically the system based on VSAT and characterizing the Ku-band channel resulting from impairments in the atmosphere. The impetus for development of VSATs is due to market demand for three systems as [2]:

1. Private data networks of low to medium traffic density.

2. Voice and data direct communication networks consisting of low response time links based on single hop.

3. Satellites making use of direct broadcast.

Most of the developed countries have seen the expansion of these new and promising systems where the terrestrial fixed optical networks and cellular systems are complemented by these systems. A vast number of applications are being developed using VSAT networks as alternative to the communications infrastructure based on terrestrial links around the globe. Ku-band offers large bandwidth and allows smaller user terminal for space crafts with spot beam antennas, which can be exploited by the next generation of satellites to allow more bandwidth. Thus, VSAT systems based on Ku-band are being developed by the satellite communications industry [4]-[5]. However, the availability of VSAT systems and the quality of transmission at these high frequencies in the Ku-band are seriously affected by the atmospheric effects [6]-[7]. Literature indicates substantial work to design efficient adaptive fading compensation methods to characterize, model and evaluate Ku-band satellite channels [8] such as variable transmission rate [9], adaptive modulation techniques [10]-[11], uplink power control [12], and adaptive forward error correction [13]. It has been found that only troposphere related impairments shall be considered for satellite links operating in Ku band above 3 *GHz* like gaseous absorption, rainfall impairments, wave refraction, multipath, scintillation and ionospheric effects can be neglected [14]. Propagation impairments on satellite signals can be caused by various weather conditions including rain, scintillation, humidity, dust and sand storms. The severity of weather conditions has an effect on how severe these impairments. For example, dust and sand storm would cause attenuation, however, severe dust and sand storm may cause satellite link outage. Rain is considered the main source of attenuation for satellite links in places like United States or Europe. In contrast, dust and sand storms are observed in different place across the globe including Saudi Arabia. So, based on the climatic conditions of the area the contributing attenuation sources vary.

2.3 Metrological Parameters Attenuating Satellite Signals

The microwave signals with wavelength close to millimetres are attenuated by our climate. The contributing factors are dust, rain, foliage sand storms etc. These metrological parameters have little impact on lower frequencies but high frequencies are attenuated by 10s of dB. Dust, rain etc introduce noise, polarization and reduce the signal strength of the wave. Efforts are made to estimate the effects of the above mentioned factors on microwaves. Different models are proposed that equate the attenuation caused by dust, rain and foliage. Figure 2.3 shows that at low frequencies, the ionosphere cannot be penetrated by radio waves and acts as a reflector. On the other hand, at high frequencies, the atmospheric gases absorb and severely attenuate the radio waves. Hence, the atmosphere provides "windows" for communications to space in which the signal attenuation increases as frequency increases [14].
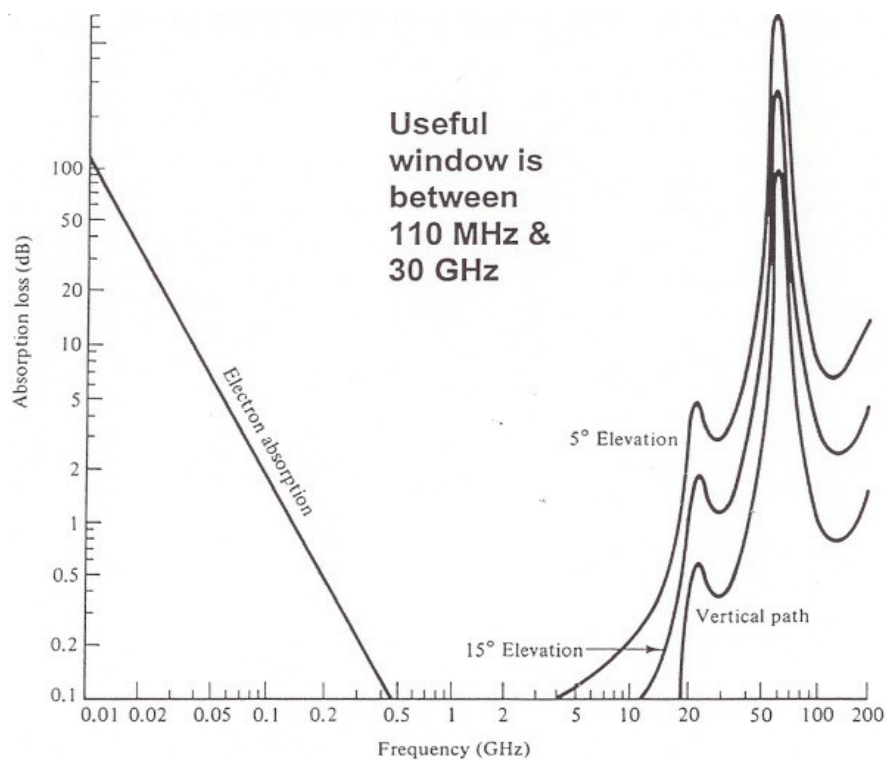
Figure 2.3: Microwave signal attenuation with respect to frequency [14].

17

2.3.1   Dust and Sand Storms

The importance of radio relay, remote sensing and satellite communication has caused much attention on the theory of sandstorm's effects on microwave propagation in the literature [15]. Usually, microwave or millimeter-wave radios are interfered by sand particles that rise above ground level to such heights due to sandstorms. This causes additional phase shift and loss in signal energy due to the absorption and scattering effect. Consequently, local area communications is interrupted and this may affect the quality of communication and coverage [16]. In temperate climates, there exit bulk refractive-index changes which triggers ducting and existence of precipitation particles, hence, producing attenuation and depolarization of the microwaves that has dominated propagation studies. However, dust and sand storms occur for significant percentages of the time especially in the Middle East, Africa, the Soviet Union and China in Asia, and some parts of South America. Such storms can affect large areas of 400-500 *km* or can be quite localized to within 10 *km*. Average durations of storms are quoted to be three hours, but durations of several hours or even days are also common. Clearly these characteristics render such phenomena as potential dangers to system reliability.

Dust is basically the sand particles suspended in air due to natural or man-made events. In deserts, winds cause dust to spread in wide regions up to 10-12 *m* high blocking the sunlight. This phenomenon is commonly known as sand storm and is common in desert planes. In order to estimate the effect of sand storm nature of sand should be studied and mathematically calculated. Sand particles are usually irregular in shape with varying sizes. Dust particles sizes can be expressed by power law probability distribution:

$$P(r) = kr^{-p}. \qquad\qquad 2.1$$

Where r is the radius of the particle, p is power law exponent, and k is selected as:

$$k \int_{r_{min}}^{r_{max}} r^{-p} \, dr = 1. \qquad\qquad 2.2$$

In [71], Rafuse calculated models for sand storms in which he claims that sand grains are maximum 0.2 *mm* in size and height of sand storms is usually $1 - 2$ *km*.

Dust storms and sandstorms are two different environmental hazards but are frequently considered alike. Drought over extended periods over an arable land causes the dust storms. As a result, fine surface particles, referred to as dust, rise up to a kilometer by strong winds. The particle diameters range from 1 to 5 micrometer. Subsequently, the sun may be obscured for the extended periods due to the fall speeds of such particles. If the visibility is smaller than one km then we classify it as a dust storm, whereas in case visibility is less than 500 *m*, the storm is classified it as a severe dust storm [17]. In one of the papers by Ghobrial and Sharief [18], a study of chemical composition of dust storms in the area of Sudan is presented which indicates 62% silicon dioxide, and 38% iron and aluminum based metallic oxides are included in the typical samples collected in Khartoum.

A sandstorm is a phenomenon in which the sand particles rarely rise higher than two meters driven by winds. The process of "saltation" is responsible for the horizontal movement of sandstorms. This is a phenomenon where the wind blows the sand particles laterally and they bounce back and forth like numerous Ping-Pong balls. The particles' diameter ranges

between 0.08 *mm* to 0.3 *mm* [19]. The chemical composition include up to 92% silicon dioxide in sand particles by weight [20]. Regions comprising of loose sand are most likely to develop sandstorms during the day at high temperatures and fizzles out at hours of low temperature [17].

Bagnold makes the distinction between dust and sand storms in one of his classic texts [21]. He describes a sand storm to comprise of thick and low altitudes and cloud where upper surface can be easily marked and the top of the sand storm is rarely higher than 2 *m* from the earth's surface with a clear air above it. Thus clearly sandstorms should not be troublesome to satellite links or to the majority of terrestrial radio relays. However, dust storms comprise much smaller particles that rise in dense clouds to a height of several thousand feet, obscuring the sun and lasting for much longer periods of time. Dust can be carried considerable distances by large storms and may not be representative of the soil types underlying the area. In some cases, at the transition of deserts and arable lands, sand storms are accompanied by highflying dust. It has also been reported that, in some parts of Africa, dust and sand storms are caused by down draughts from summer thunderstorms and by the passage of cold, fronts during winter: In tropical areas, where humidity is high, a certain amount of moisture m will also represent the dust and sand particles. Various transmission parameters like refractive index and electromagnetic scatter of the dust and sand particles are changed due to the moisture affecting the quality of transmission [21].

Various researchers have studied sandstorms and the results have been reported for their effects on the amount of attenuation and phase shift on signals in upper band [22]-[23]. There are few publications on dust and sand storms' effects on microwave propagation due to moisture content, visibility and particle size distribution [24]-[25]. In another paper, Chen et al. investigated the microwaves' attenuation in heavy dust and sand conditions based on the

turning bands and finite difference time-domain methods [26]. Further, it has been revealed that the sand particles' shape is responsible for the attenuation, cross polarization and phase shift once microwaves propagate in dust and sand storms [27]-[28]. These works have specifically reported the results taking into account the spherical and elliptical sand/dust particles. Attenuation formulas for polarized wave propagation in both vertical and horizontal directions have been derived by Ghobrial and Sharief in [27] at 10 *GHz* in dust storms. Effects of particle size distribution on microwave propagation in mud storms have been dealt by Ahmed [29]. McEwan and Bashir [30]-[31], Salmaen et al. [32], Ghobrial and Sharief [27] and other researchers [28]-[33] have investigated the cross polarization phenomenon due to dust.

To simplify the problem involving randomly distributed sand/dust particles, Q. Dong et al. have used the relationship of optical visibility and total relative volume [15]. Using the Rayleigh approximation for the particles' forward scattering amplitude, the general formula to model the microwave propagation in storms as a function of frequency and expressions for differential phase, shift and attenuation for polarizations in orthogonal directions have been developed. Also, the effects of visibility, moisture content, frequency and particle shape on microwave attenuation are discussed. The values obtained from the derived equations are in harmony with those obtained by classical Ghobrial's and Goldhirsh's formula.

Microwave open-resonator techniques have been used in recent years in order to obtain refractive-index data. Ahmed and Auchterlonie [34], have made measurements at 10 *GHz*, and Chu [35] has used these in order to predict attenuation data bounds at 10 *GHz*. Ghobrialet al. [18] has attempted a similar prediction using a different method and have also highlighted the effects of moisture on the refractive index [36]. Another paper by Al Hafidet reports calculations and some experimental results taken in Iraq [37]. The experimental results show

much greater attenuation than predicted by theory. A characteristic of the works to date is that calculation has only been performed to around 10 *GHz*, and this is mainly due to the lack of information on dielectric constant, and hence refractive index at the higher microwave frequencies. In addition, it appears that only attenuation has been calculated and, although this is undeniably the most significant transmission parameter, modern radio systems are increasingly using dual polarization, and hence cross-polarization is also of interest. Hence, in order to calculate the transmission parameters, one must have knowledge of the particles' shape and orientation as well as the size distribution and refractive index needed for the attenuation calculation. The calculation of transmission parameters in sand or dust storms parallels that of the calculation in rain or ice, which has been fairly well documented in the literature [38].

Authors in [39] present the results of a study aimed at answering the questions including:

1. What data exist for basic particles?

2. Is the Rayleigh approximation valid or do we need to adopt exact scattering methods?

3. Is the medium modeling satisfactory?

The theoretical prediction of propagation in precipitation conditions has received much attention in the literature where in some parts of the world dust and sand storms occur more frequently. To answer these questions, the authors attempted to place bounds on the likely depolarization and attenuation in the 3-37 *GHz* frequency range covering most of the existing and planned operational radio and satellite links. It is shown that attenuation and cross-polarization effects are quite small in modest dry dust and sand storms with visibilities around 100 *m* for linear polarization up to 37 *GHz*. However, significant attenuation and

cross-polarization can result in humid areas for circular polarization, and bad storms with visibilities around 20 *m* or less.

Most researches assumed a uniform distribution or a specific geometric shape for DUSA. This approximation is providing appropriate results for medium to high visibility, yet, providing inaccurate estimation during severe dust storms with low visibility. DUSA was under intensive study in KSA for so many years. Researches [40]-[41] have derived different formulas to model this complex metrological parameter. The complexity is due to the conduct and structure of dust and sand storms which look to be uncorrelated from one region to another due to the non-uniformity of the dust characteristics and several other atmospheric factors.

Various authors have reported that the severity becomes increasingly debilitating at the higher ends of the high frequencies [42]-[44]. Consequently, satellite-dependent resources affected by weather are extremely hard to optimally manage. It is argued that an effective technical solution to significantly improve the QoS will depend on the ability to properly identify, predict, and qualify the overall impact of individual attenuation factors. Methodologies that attempt to combine them in a cohesive manner are not widely available in spite of availability of a number of models for dust and sand storm attenuations for estimating individual attenuation components.

A special case of approximated dust distribution of ellipse shape of the dust storm has been described by the Authors of [45]. Another case, the vertical variation of the dust storm has been modeled by authors of [46] based on the idea that the visibility is directly proportional to height. In [41], the vertical path adjustment factor has been estimated by the authors according to the specific shape of dust storm. A new approach for determining visibility

based on dust storm model has been presented in [38] as well as a new method to slice the dust storm into multiple sections depending on discrepancies in visibility at different heights.

History shows that the defense organizations have remained the flag bearers in carrying out latest research in various science fields including the space science domain. This is because the defense doctrine is transforming to an expanded, more mobile battlefield, which is creating an ever-increasing demand for bandwidth and mobility. To address the defense requirements to meet the demands for bandwidth and mobility, the Wideband Gapfiller System has been developed to provide a high capacity Ku-band transponder. However the Gapfiller payload is truly a wideband system that has an inherently limited capability to support small aperture terminals, particularly on the downlink where satellite radiated noise may have a limiting effect on small signal links [47].

Moreover, the impact of dust and foliage on signal propagation has been discussed by the authors in [48]. They have presented the experimental statistics and models to characterize dust and foliage attenuation. Link degradations on the order of 0.1 dB have been found due to sand and/or dust which are smaller but have 3-4 dB per meter of foliage which is quite high. They have concluded that communications in the millimeter wave range through any length of foliage should only be encouraged if operational adjustments and mitigation procedures exist whereas adequate link design is necessary through a dust laden communications path.

There are various other factors like soil texture, optical visibility, distribution of dust particles' size and relative humidity which may considerably affect high frequency waves in dust and sand storms apart from causing significant back scatter and signal attenuation. The effects of relative humidity to predict millimeter waves' attenuation during dust and sand storms in dry regions and soil textural class are presented in [49]. The authors have found that

24

these waves are generally affected by the dry clay particles more than the dry sand. However, as the moistness of dust and sand particles rises, these waves are more severely affected. Various other papers report measurements for dust and sand dielectric constants. An open cavity technique is used by Ahmed and Auchterlonie [50] to compute dielectric constant values of dry sand and clay. Further, Ghobrial [51] established a fact that dielectric constant is different for individual samples due to the different chemical compositions and varying water content. Sharief and Ghobrial investigated the effects of chemical constituents, frequency and humidity on microwaves [52]. Using microscopic measurements and assuming dust particles to be elliptical with same average axes ratios, McEwan and Bashir [30] computed the cross-polarization of sand particles and presented results in terms of the relative volume of dust. In [53], axes ratios based statistical theory is developed and results are given in terms of visibility and the dust per unit volume is not considered. The authors state that visibility can be measured to determine the storm severity and define the difference between sand and clay based on particle's radius. As per the authors, the airborne particles of sizes up to 60 micron are termed as dust particles and incorporate the clay particles. Thus, airborne particles of size greater than 60 micron are referred to as sand.

J. Goldhirshhas reviewed the fundamentals of radar backscatter and attenuation through dust storms in [54] by modeling a dust storm as circularly symmetric with minimum visibility at its center, improving exponentially in radial direction to maximum. Path attenuation and radar backscatter are then conveniently calculated using dust storm model. The experimental results carried out in Sudan showed backscatter and attenuation levels to be relatively negligible for frequencies up to 10 *GHz* even in intense dust storms.

2.3.2 Foliage

Of all the geological attenuating factors, foliage is difficult to estimate. Due to the different types and densities of foliage makes this attenuation greatly variable. Most of the studies conducted on foliage cover the horizontal signal propagation with lower frequency bands.

Currie, et al., has generated the most useful data for such impairment [21]-[23] at discrete different frequencies up to 90 *GHz*. Radar methods were exploited to collect the data, using a corner reflector object fixed in the foliage and measuring the attenuation. The foliage attenuation has been approximated per meter of path length by the following expression:

$$a\left(\frac{dB}{m}\right) = 1.102 + 1.48log_{10}(f). \qquad\qquad 2.3$$

The foliage attenuation is hard to precisely quantify. However, it is also clear that foliage attenuation can severely degrade, and potentially preclude, satellite communications in the millimeter regime regardless of the available link margin.

2.3.3 Rain

One of the principal causes of signal attenuation in satellite communications is recognized as rain between 3 and 300 *GHz* range. This phenomenon is termed as "rain fade" where signal degradation occurs in proportion to the amount of rainfall. Higher frequencies are more susceptible to rain fades as Ku band may encounter 3-5 dB/sec power drop in comparison to C-band rain fade around 1 dB/sec. Some rain characteristics may cause attenuation in the order of multiple dBs. The effect of rain on satellite communications link performance has been quantified by many researchers [48], [55]-[61].

A. A. Lotfi-Neyestanak, BabakMirzapour and M. Jahanbakhtstress to employ propagation models based on statistical description of rain rate to predict path attenuation for designing communication links and radars [55]. The authors in [56] highlighted that old climate data sets are being used for the modeling of rain rate probability distribution that are not valid for many regions of the world. It is found that rainwater attenuate electromagnetic waves in the lower troposphere. A couple of papers show that the satellite links operating at frequencies above 6 *GHz* are significantly impacted by path attenuation [57], [58]. In Taiwan, Chen and Chu investigated the transmission performance of a multipoint distribution system operating at Ku band with quadrature amplitude modulation [59]. A set of revised International Telecommunication Union (ITU) models for rain attenuation satellite links from earth to space are generated exploiting the measured data collected different regions in [60], [61]. These modified models take cumulative distribution of rainfall rate as input and show improved results for the existing attenuation models. In [62], authors presented computations of satellite signal attenuation in Fiji due to tropical weather.

Data related to 1-minute integrated rain rate gathered from Colombia is used for empirical cumulative distribution function for the worst month in [63] and further utilized for future rain prediction. Another approach derives an analytical relationship between the rain-attenuation effects and the Ricean K-factor in [64]. To estimate reflectivity and attenuation observations at 35 *GHz*, a simple microphysical precipitation model is developed using thermodynamic phase state and hydrometeor size distributions [65]. There are always some undetermined parameters that are required for the perfect rain attenuation modeling at various localities. Keeping above in mind, climatology skills are used by the author in [55] to identify similar meteorological areas in different countries and generalization of the rain-rate attenuation prediction model. The benchmark method is also analyzed to establish the accuracy of the results obtained by the proposed method.

A two-wavelength technique can be implemented with single radar for W and Ku band radars and are less sensitive to attenuation of radiation in precipitation and clouds. This is because of the fact that differences in attenuation are weaker than resonance scattering effects. As a result, information on scattering particles can be inferred due to scattering resonance effects on droplet by taking measurements at two different wavelengths [66]. Another work focuses on rain fade which suggests ways to compensate the QoS during this time in India using 16 spot beams [67]. The authors in [15] have formulated the wave propagation constant based on the sand/dust particle's forward scattering amplitude using the Rayleigh approximation. Moreover, general equations for phase shift and attenuation coefficients are also developed.

An ITU-R model is developed to estimate the rain effects on frequencies ranging above 10 *GHz*. A vast research is done to further improve the ITU-R model. Due to sandy plains and very less occurrence of rain, it is not point of interest in region of Saudi Arabia [75].

2.4   DVB VSAT Systems

2.4.1   Introduction

Satellite are commonly used for communication and real time data transfer from when one point to other. There are many other modes of communications which are proven fast and reliable but satellite are very much effective when the communication is over very large distance i.e. from one continent to another. Satellite communication is also effective in remote location where deploying a complete network is not feasible. The general concept of VSAT is shown in Figure 2.4.
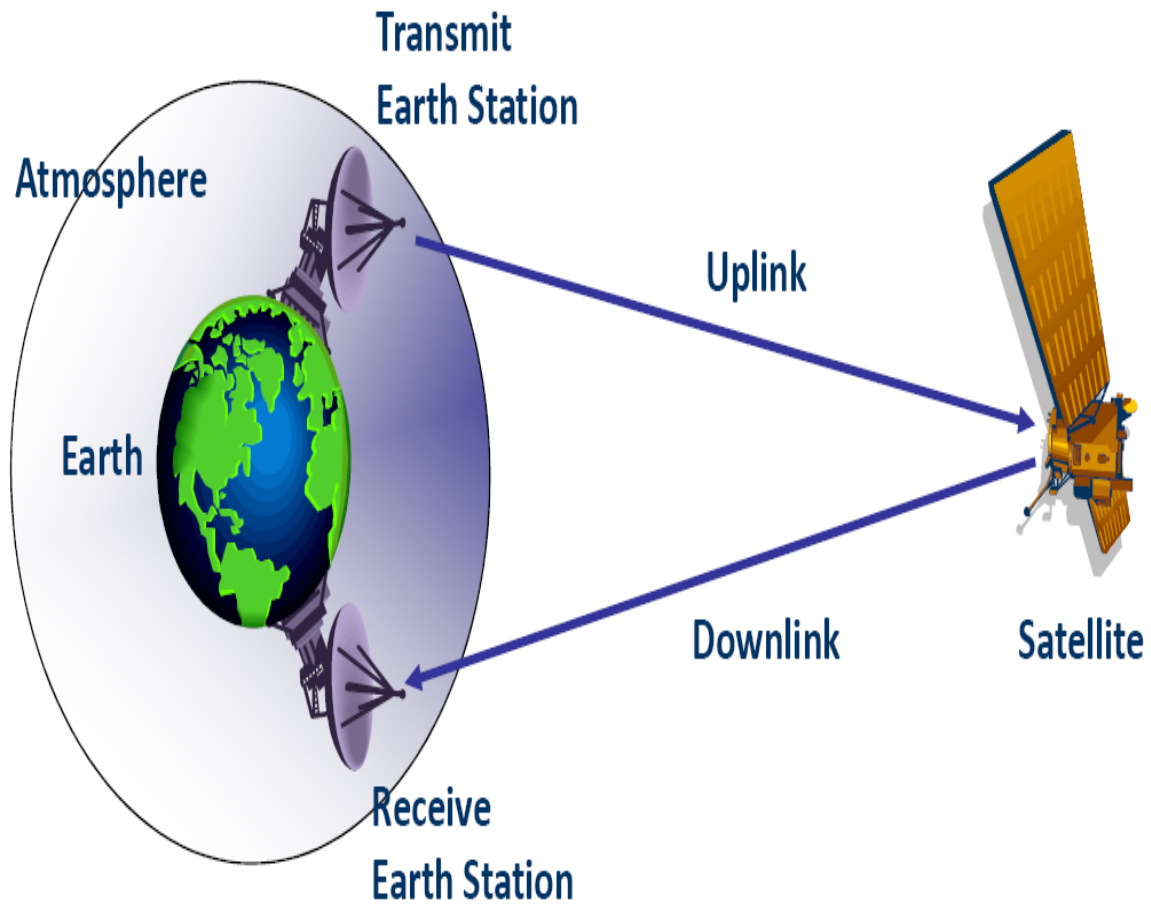
Figure 2.4: Basic principle of a VSAT system.

A typical VSAT terminal consists of two parts namely the indoor unit (IDU) and the outdoor unit (ODU). The ODU consists of a block up-converter (BUC), low noise block-down converter (LNB), feed horn and satellite dish as shown in Figure 2.5.
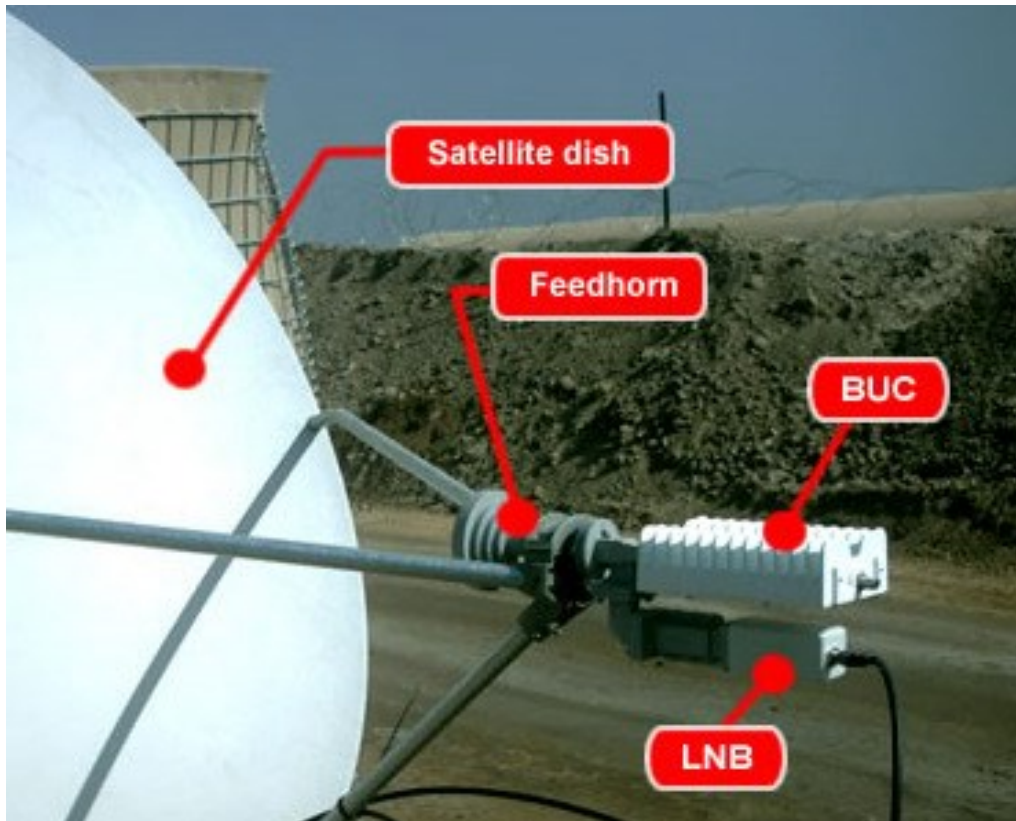
Figure 2.5: Typical VSAT terminal ODU.

A BUC is a combination of an up-converter and a high power amplifier (HPA), and is typically mounted right on the feed of an antenna. It is typically used for lower-cost or lower size applications since the size of the BUC that can be feed mounted is limited. An LNB is a combination of an LNA and a down-converter. It is typically mounted right on the feed of an antenna. It is typically used as a cost-saving measure, but the performance of LNB is typically somewhat worse. LNBs directly mounted to feed have better performance than side-mounted LNBs.

The IDU consists mainly of a modem as shown in Figure 2.6.

Figure 2.6: Sample modem "SatNet S5300 IDU".

A MODEM is an abbreviation for modulator and demodulator. A modulator converts a baseband digital signal into analog form compatible with the satellite channel. A demodulator converts the analog signal back into the digital baseband signal.

Modern modems also include other functions:

- **Amplification:** the signal is amplified to a level suitable for further processing and for driving the next stage.

- **Terrestrial Interfaces:** modems include digital interfaces to interface with other terrestrial equipment, e.g., routers.

- **Upconverters:** at the transmitter, the output signal from the modulator is usually converted to an intermediate frequency (IF) – typically 70 *MHz* or 140 *MHz*.

- **Downconverters:** at the receiver, the signal is converted from IF to baseband.

- **Error control coding:** at the digital data stream is encoded to guard against errors during transmission; at the receiver, the data stream is decoded.

2.4.2   Orbits

Satellites revolve around the earth at very far locations called orbits. Based on the distance and parameters there are basically three orbits in which satellites can revolve. Each orbit has

its pros and cons and is being used to achieve a specific goal. Table 2.1 below compares the three orbits.

Table 2.1: Comparison of satellite orbitals.

	LEO	MEO	GEO
Description	Low Earth Orbit	Medium Earth Orbit	Geostationary Earth Orbit
Height	$500 - 1,500$ *km*	$5,000 - 18,000$ *km*	$35,863$ *km*
Satellite Velocity	$7.1 - 7.6$ *km/s*	$4.0 - 5.9$ *km/s*	3.1 *km/s*
Time in Line of Sight	15 *min*	$2 - 4$ *hrs*	24 *hrs*
Merits	Lower launch costs Very short round trip Small path loss	Moderate launch cost Small roundtrip delay	Covers 42.2% of the earth's surface Constant view No problems due to Doppler Effect
Demerits	1. Shorter life 2. Encounters radiation belts 3. Fast tracking, intermittent visibility 4. Satellite switching	1. Larger delays 2. Greater path loss 3. Satellite tracking, intermittent visibility 4. Satellite switching	1. Very large round trip delays 2. Expensive Earth Station due to weak signal

2.4.1   DVB Standards

2.4.3.1   DVB-RCS

The DVB-RCS specification (ETSI EN 301 790) was advanced for multiple years. It was meant to have excellent burst and frame efficiencies. To acquire such efficiencies, an aggressive short preamble burst structure ever implemented in a multi-frequency time division multiple access (MF TDMA) system was proposed by the standard. Latest in carrier frequency and symbol timing recovery techniques have been used to achieve the required aggressiveness. Further, the initial specification determined a technique that was designated "Fast Hop" which clearly specified an ability to hop between two adjacent bursts, within a designated guard band (section 6.7.1.3 of EN 301 790). In later evolutions of the specification, a major effort was made to reduce the cost of DVB-RCS terminals, whilst retaining the high frame and burst efficiencies that were the hallmark of a DVB-RCS system. This effort resulted in the designation of "Slow Hop" (section 6.7.1.3 of EN 301 790) which allowed the terminal to take a full traffic (TRF) burst to settle when moving across the designated MF TDMA frequency range. This method was anticipated to have minimal impact on the capability and performance of the terminal, whilst allowing a major reduction in the cost and complexity of the terminal hardware.

2.4.3.2   DVB-S2

DVB-S2 VSAT stands for digital video broadcasting via satellite second generation. It is currently the latest satellite communications standard in production and is commonly used for video based applications. It has the feature of low encoding complexity and also has variable and adaptive coding and modulation modes which can be used for fluctuating noise conditions. It provides enhanced data rate than DVB-S1. The DVB-S2 specification (EN 302 307) specifies a number of modes of transmission adaptation. These are:

1. Adaptive Code and Modulation (ACM).

2. Constant Code and Modulation (CCM).

3. Variable Code and Modulation (VCM).

The primary use of VCM is to support multiple services levels on the same carrier or to compensate for different propagation characteristics across a service area on the same carrier. An example of this technique is to use one combination of modulation and coding for the edge of coverage and another for the center of the satellite beam. The satellite coverage is fairly uniform across Saudi Arabia with approximately 1-2 dB of change from the center of coverage to the most southern area. Using VCM in this case could have an advantage to provide a more uniform level of service. Another possible use of VCM involves the fixed and fixed back-up terminals. These have larger antennas than the auto-acquisition and stabilized terminals. Therefore they can operate with a higher order forward error correction (FEC) coding than the other terminals. This results in a savings on the forward link bandwidth. Saudi Aramco VSAT system implements the broadcast services (BS) version of the DVB-S2 specification and supports CCM.

2.4.3.3   Saudi Aramco VSAT System

The DVB-RCS based VSAT system utilized in this study uses the most advanced modulation and coding on the forward (gateway to remote) and return (remote to gateway) satellite links available in the DVB-RCS specification.

In the return direction, the system uses QPSK modulation with Turbo coding as per EN 301 790 exclusively. The system offers a variety of Turbo coding rates depending on the nature of encapsulation chosen for the return traffic. Table 2.2 summarizes the performance of the return link.

Table 2.2: Spectral efficiency DVB-RCS return link.

Turbo Coding (rate)	Channel Spacing Factor	Spectral Efficiency (Bits/sec/Hz)
1/3	1.25	0.53
2/5	1.25	0.64
½	1.25	0.80
2/3	1.25	1.07
¾	1.25	1.20
4/5	1.25	1.28
6/7	1.25	1.37

Studies with simulations as well as extensive practical experience in hundreds of deployments concluded that Turbo code rate 2/3 provides the optimum balance between spectral efficiency and coding gain. As a consequence, Turbo coding rate 2/3 is being exploited in all return links in the Saudi Aramco VSAT network.

In the forward direction, the system uses DVB-S2 in accordance with the DVB-RCS specification EN 301 790. It offers both QPSK and 8PSK modulation schemes for its forward links. While 16APSK and 32APSK modulation schemes are matched to broadband VSAT applications which is not the case in Saudi Aramco network. 32APSK and high coding rates of 16APSK require large signal-to-noise ratios (SNR) greater than 12 dB. Please refer to Figure 2.7 below which depicts the E_s/N_0 versus spectral efficiency for the various modulation schemes. While these signal-to-noise ratios are readily achievable for trunking applications between large earth stations, they are not generally available for VSAT networks. The network operator can dramatically increase the forward link equivalent isotropically radiated power (EIRP) from the hub station to get the required signal to noise at the VSAT remote terminal but is likely to consume more satellite power than bandwidth.

This defeat the advantage of the narrow bandwidth because the satellite operator will base his tariffs on the larger of the power or bandwidth used. Alternately the network operator can increase the size of the VSAT remote terminal antenna. With this approach, however, the network operator loses the portability of the terminals and cannot support applications requiring stabilized platforms or auto deployed antennas.

In summary, the only practical modulation schemes for the DVB-S2 forward link carrier in VSAT networks are QPSK, 8PSK and 16APSK using low rate codes. 32APSK and 16APSK with high rate codes are better suited to trunking applications between larger earth stations. This crossover point is readily evident in Figure 2.7 below. Note the spectral efficiency is expressed as bits/symbol. The bits/Hz efficiency can be determined by adjusting the bits/symbol efficiency by the roll off factor. Saudi Aramco VSAT network supports 20%, 25% and 35% roll off factors.
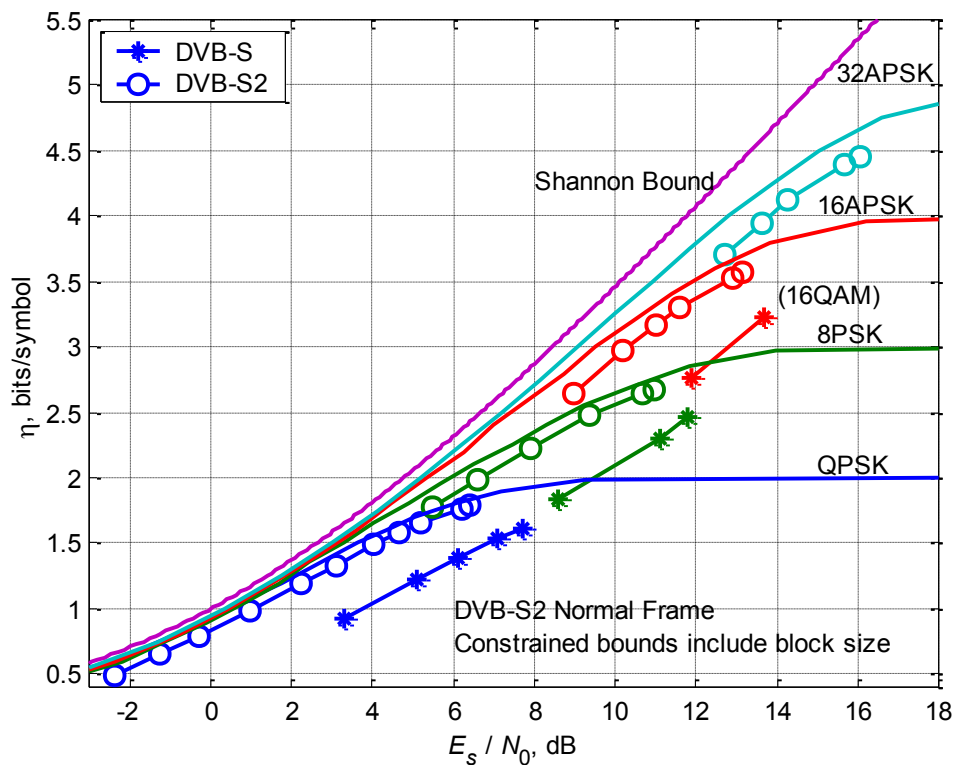
Figure 2.7: Spectral efficiency of DVB-S2 modulation schemes.

2.5   Antenna Design

Long distance radio communications requires high gain antennas. Reflector antennas are most widely used for long distance communication which can easily achieve gain of 30 dB. The first reflective antenna was designed by Hertz in 1888 based on principal of geometrical optics.

The antenna is composed of two components, the reflecting surface and small feed antenna. Based on geographical and industrial demand they could be different in shape. Commonly used shape is the parabolic antenna. Other could be cylindrical, spherical and corner reflectors.

The operation concept of a parabolic antenna is that the signal is injected at the feed which is placed at the focal point of the reflector. The reflector reflects the signal in the direction of boresight – which is pointed towards the satellite. The larger the antenna, the better the ability to concentrate the power, i.e., the higher the apparent gain. The power is not all concentrated in the main beam rather much of it is lost in spurious transmissions in other directions. The higher the efficiency of an antenna, the more the useful power, i.e., the higher the gain. Gain of commonly used parabolic reflector antenna is as below:

$$G = \frac{4\pi A}{\lambda^2} e_A = \frac{\pi^2 d^2}{\lambda^2} e_A \, . \qquad\qquad 2.4$$

A is the area of the antenna aperture.

d is the diameter of the parabolic reflector.

λ is the wavelength.

e_A is the antenna efficiency. The typical value is between 0.55 and 0.70 depending on the materials quality.

2.6   Modulation Schemes in VSAT Networks

VSAT systems commonly use PSK modulation schemes due to the fact that it has the advantage of a constant envelope compared to the FSK modulation scheme. Hence, provides better spectral efficiency.

The most common schemes used schemes are as follows:

- Binary phase shift keying (BPSK).

- Quadrature phase shift keying (QPSK).

- 8 Phase shift keying (8 PSK).

- Quadrature amplitude modulation (QAM).

- Amplitude phase shift keying (APSK).

Based on link condition that is SNR, VSAT could adapt to any of the above scheme. Long distance and environment cause inference in the communicating signal which cause error in the received message. Error correction techniques are widely used in order to correct the data and save retries. Error correction techniques also help to achieve high data rates in real time environment. Commonly used error correction techniques in VSAT are as follows

- Convolution codes with veterbi algorithm.

- Reed solomn (RS) codes with interleaving.

- Turbo codes.

- Low density party check (LDPC) coding.

CHAPTER 3

ESTIMATION OF DUST AND SAND ON SATELLITE COMMUNICATIONS LINK

In the previous chapter, we have studied in detail the metrological parameters which affect the communication channel. In prospect of Saudi Arabia, dust and sand storms are the major sources contributing to the random behavior of a satellite communications channel. So, our focus in this study is on models that simulate effects of dust and sand storms on the high frequency (Ku band) satellite links.

3.1 Rayleigh Approximation

In [15], considering backward scattering amplitude for particle under the Rayleigh approximation, empirical formulas of the wave propagation constant through dust and sand storms were developed. For a medium with dust and sand particles, the phase shift and attenuation coefficients are derived in terms of frequency and visibility. By following the analysis, the propagation based on particles slab model is:

$$K_{V,H}(\varphi) = k_o + \frac{2\pi}{k_o} \int_0^\infty f_{V,H}(\varphi,r)N(r)dr \, .$$ 3.1

Where k_o represents free-space propagation constant, φ is the incident radiation elevation angle and $N(r) = N_0 P(r)$ is the per unit volume particle size distribution having radii in the region $r \rightarrow r + dr$. $f_{V,H}(\varphi, r)$ represents the vertical and horizontal polarizations of the backward scattering amplitude, as depicted by the symbols V and H.

3.2   Goldhirsh Derivation

Assuming a Rayleigh approximation, the dust and sand storms attenuation model for microwave propagation derived by Goldhirsh and can be expressed as [15]:

$$a = \frac{2.317 * 10^{-3} * \varepsilon''}{[(\varepsilon' + 2) + \varepsilon''^2] * \lambda} * \left(\frac{1}{V_b^{\gamma}}\right). \qquad 3.2$$

Here λ is the wavelength in meters, V_b is the visibility in kilometers, ε' and ε'' are the real and imaginary part of the complex dielectric constant of the dust particle and γ is a constant equal to 1.07.

3.3   Ahmed et al. Derivation

Ahmed et al. proposed a dust and sand storms attenuation model for millimeter-wave propagation exploiting Mie scattering theory and measured probability density function and is expressed as [15]:

$$\alpha = 5.670 * 10^4 \frac{1}{V_b} \left(\frac{r_e}{\lambda}\right) \frac{\varepsilon''}{[(\varepsilon'' + 2) + \varepsilon''^2]}. \qquad 3.3$$

Here r_e is the radius of the particle in micrometers.

3.4   Ahmed Derivation

Assuming the Rayleigh approximation, Ahmed derived dust and sand storms attenuation model tailored to any particle size distribution which can be expressed by [15]:

$$\alpha = 0.629 * 10^3 \frac{Fr_e}{V_b} \frac{\varepsilon''}{[(\varepsilon'+2)+\varepsilon''^2]}.$$

3.4

Where F is frequency in GHz.

3.5   Al-Haider Derivation

Considering ten years visibility data and the Rayleigh approximation, a model for dust and sand storms attenuation has been derived by Al-Haider which can be expressed as [15]:

$$\alpha = \frac{0.189}{V_b} \frac{r}{\lambda} \frac{3\varepsilon''}{[(\varepsilon'+2)+\varepsilon''^2]}.$$

3.5

Where r is the radius of the particle in m.

A comparison of dust and sand storm values with above mentioned existing models in literature is shown in Figure 3.1.
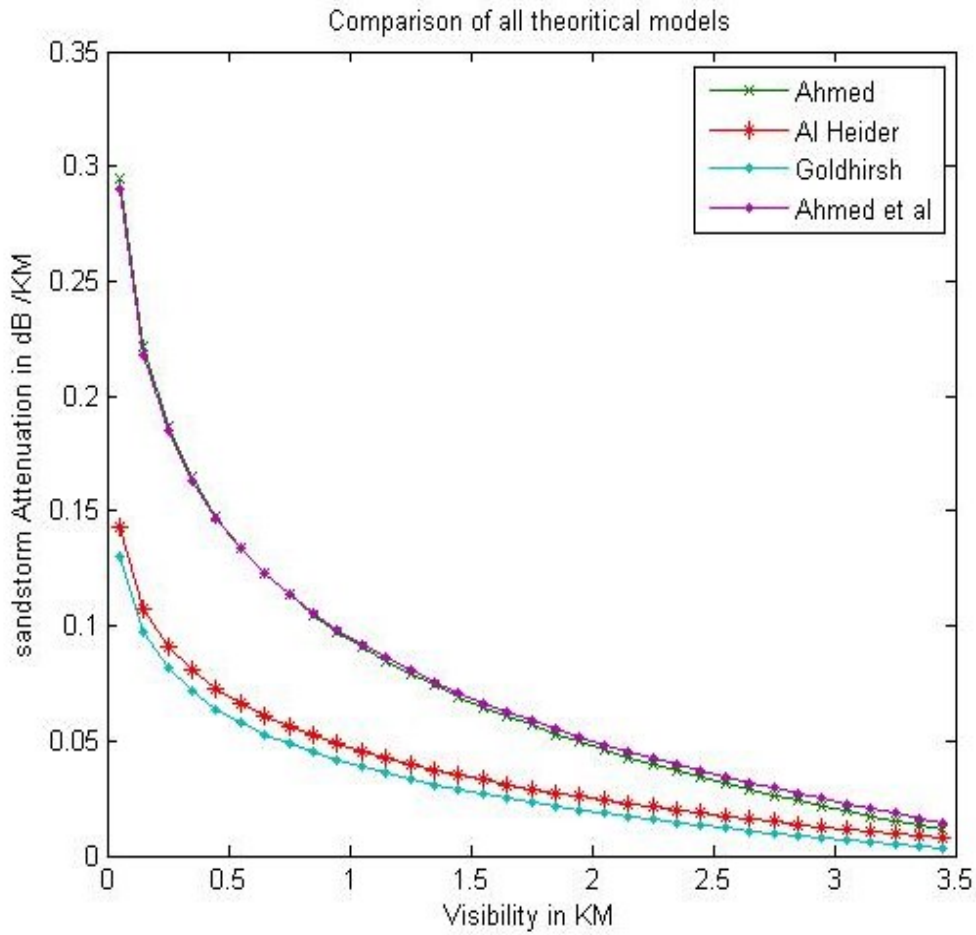
Figure 3.1: Comparison of DUSA models derived by Goldhirsh, Ahmed et al., and Al-Haider.

Figure 3.2 and Figure 3.3 extracted from [15] show the relationship between the visibility and attenuation at $F = 37$ GHz and 24 GHz. The dielectric constants of dust for both cases have been assumed to be $\varepsilon_m^* = 4.0 - j1.3$ and $\varepsilon_m^* = 5.1 - j1.4$, respectively. The graphs revealed that the attenuation increases as the moisture content and frequency increase.
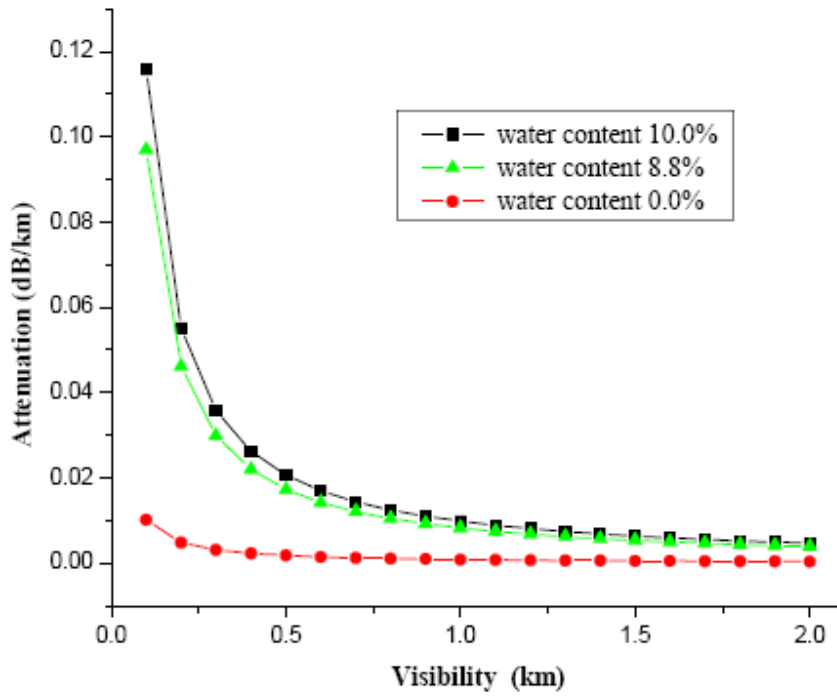
Figure 3.2: Attenuation for different moisture contents.
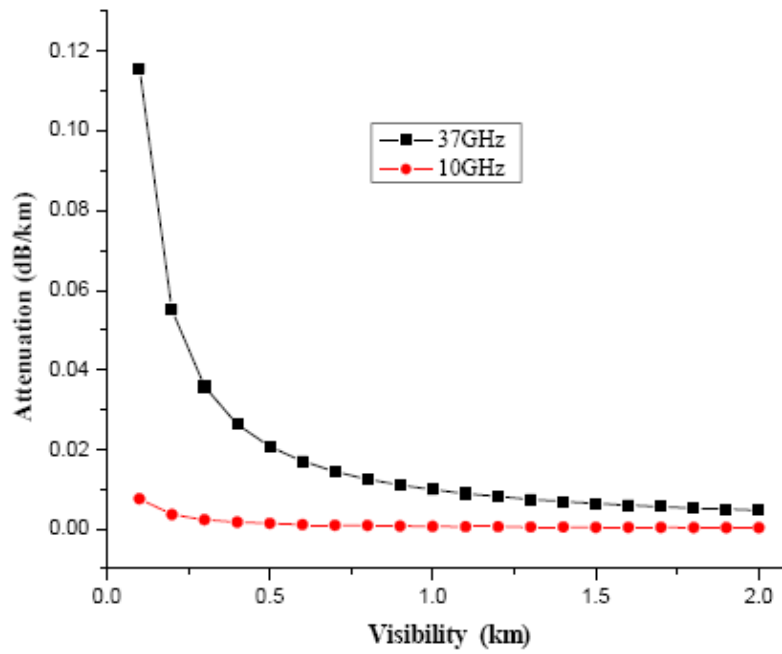
Figure 3.3: Attenuation vs visibility at different frequencies.

CHAPTER 4

CALCULATIONS OF DUST AND SAND

ATTENUATIONS

In this chapter, a methodology is formulated for estimating dust and sand attenuations based on latest techniques available in literature and incorporating metrological data obtained from physical measurements. The effect of dust and sand storms on Ku-Band DVB-S2 VSAT networks in the region of Dhahran, Saudi Arabia is studied. Prediction of attenuation on satellite signals due to dust and sand storms is the sole objective of this chapter.

4.1   Experimental Setup

4.1.1   VSAT Network

In cooperation with Satellite Solutions and VSAT Support Groups, the own VSAT system by Saudi Aramco has been exploited to conduct all required testing for this thesis work. A top-level diagram of the VSAT network exploited in the testing is shown in Figure 4.1. This shows two gateway sites, one at Tanajib that contains the first gateway for half the terminal population (sub-network 1) and the second Gateway, at Haradh, for the other half of the terminal population (sub-network 2).
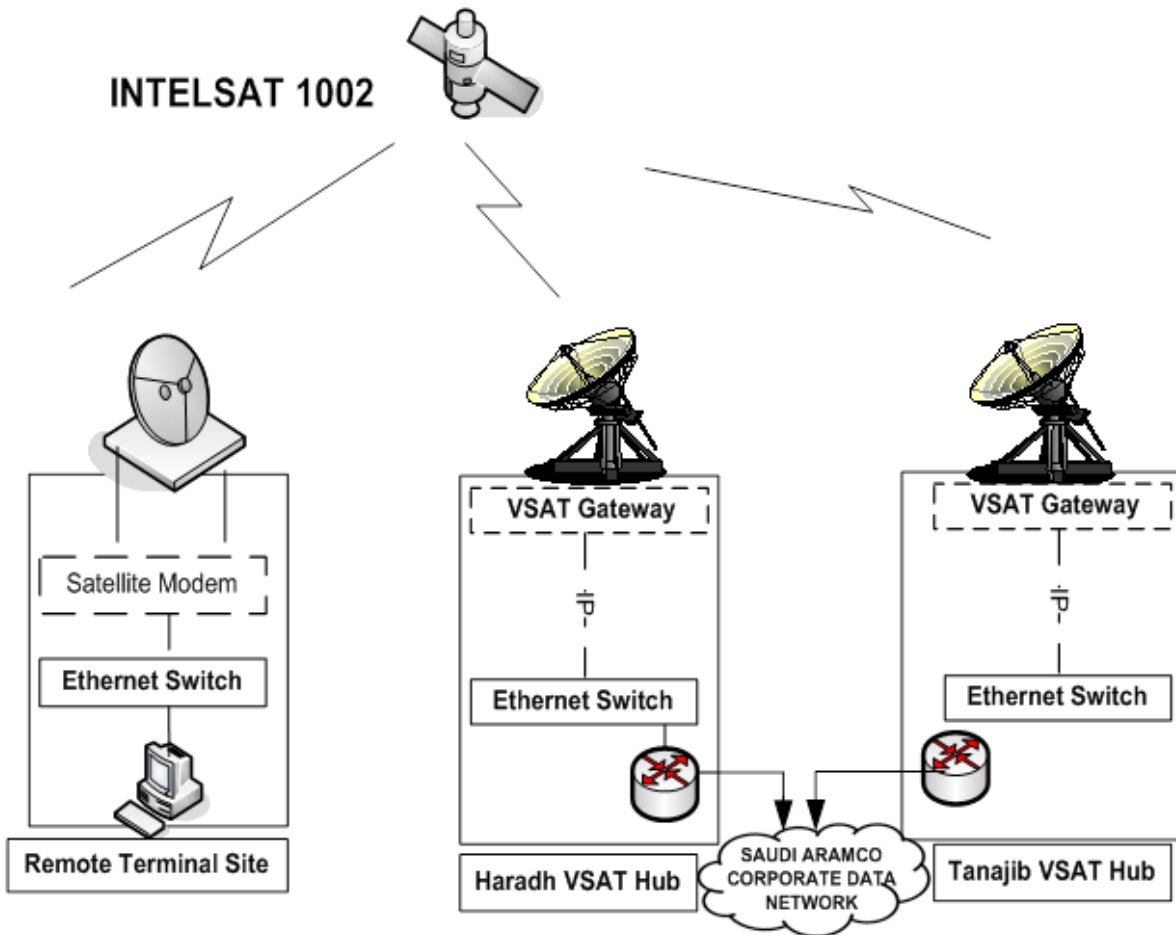
Figure 4.1: VSAT network diagram.

Data traffic in all cases terminates/originates to/from the Saudi Aramco backbone routers and telephone switches located at the two gateway locations. This design supports data communication between a remote in one sub-network and Saudi Aramco network, between two remotes in one sub-network and between two remotes in a different sub-network (one remote in sub-network 1 and one remote in sub-network 2).

The space segment of the VSAT network consists of two transponders on Intelsat 1002. The allocation of resources is done in a way to devote one transponder to the forward link and return link of one gateway and the other transponder to the forward link and return link of the other gateway as shown in Figure 4.2.
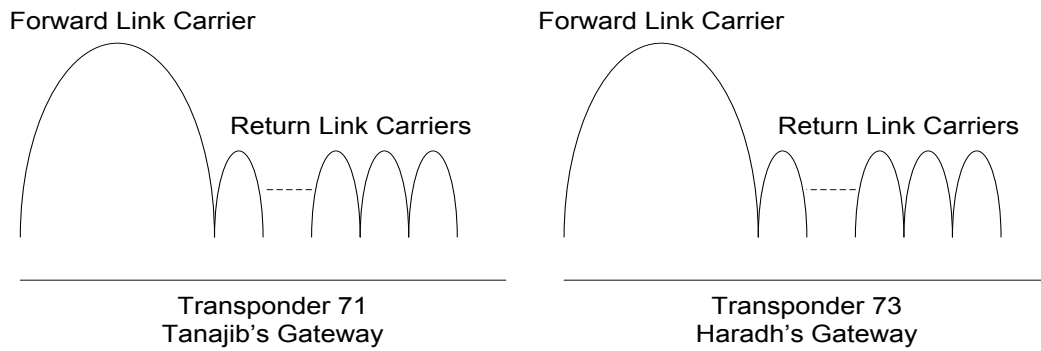
Figure 4.2: Transponders Frequency Plans.

4.1.2 Test Bed

The test setup mainly consists of a VSAT remote terminal and a visibility sensor both located in Dhahran. The SNR of the transmitted data is physically measured to quantify the effects of such factors on the composite attenuation. Also, the visibility was observed at the same time. A sample of the data collected is shown in Appendix I.

Initial assessment for the data collected shows that:

- Based on the observation data, 109 out of 647 records showed SNR below the threshold of 6.5 dB.

- Link outage given that there is sandstorm = 109/647 = 0.168.

- Observation time span = 10 *min*.

- Probability of dust and sand storms in the region total time frame = 2 *yrs*.

- Probability of sandstorm in terms of total time = 100* (109*10) /(2*365*24*60) = 0.1%.

- Maximum system reliability is 99.9% (100 - 0.1).

- So, the system typically experiences link outage = (0.1* 60*24*365/100) = 525 *min* per year

- Designed system reliability percentage is 99.95%.

- Designed system outage in time is 262 *min*.

- Additional System Outage due to heavy Sandstorm: 263 *min*.

4.1.2.1   VSAT Remote Terminal

Figure 4.3 and Figure 4.4 show the IDU and ODU of the remote terminal used in the test setup. Figure 4.3 shows the DVB-RCS indoor unit (IDU) used which is the SatNet S5300 IDU. This is Advantech satellite networks' fifth generation of DVB-RCS modem and includes the most advanced features available. The SatNet S5300 IDU incorporates the DVB-S. Additional capacity and adaptability will be built into the unit as follows:

- Ability to handle higher power BUCs.

- Wider symbol rate range on the forward link.

Table 4.1 shows the technical specifications of the IDU used in the test.

Table 4.1: SatNet S5300 IDU performance capabilities.

Parameter	Performance
Data Rates:	Forward Link: DVB-S 1–45 MBaud DVB-S2 1–30 MBaud Return Link: 128 kb/s – 4 Mb/s
Air Interface Forward Link:	DVB-S (EN 300 421); QPSK, code rates 1/2–7/8 DVB-S2 CCM (EN 302 307): Normal frames, QPSK, LDPC code rates 1/2–9/10, 8PSK rate 2/3–9/10, roll-off 1.2–1.35. Encapsulation: IP over MPEG (MPE)
Air Interface Return Link:	DVB-RCS (EN 301 790); QPSK, Turbo code (TCC) rates 1/2–6/7 for traffic, 1/3-6/7 for signalling Encapsulation: DVB-RCS: IP over ATM (VC-MUX), IP over MPEG (MPE)
Physical Interfaces:	ODU/IFL: L-band, dual cable, F-type connectors Network: 10/100 Base T, RF45 connector
ODU Support:	Up to 4W BUC Transmit frequency bands: Ka, Ku, C, Offset-Ku (Option) Receive frequency bands: Ka, Ku, C
Management:	Local GUI (Web browser based) SNMP; Advantech / DVB-RCS MIB
Installation Support:	Advantech FLCM
Power supply:	100–240 VAC 50–60 Hz

Figure 4.4 shows the ODU used in the test which constitute of an antenna, BUC and LNA from AvL technologies. The ODU different components technical specifications are show in Table 4.2. The antenna receives a signal from the satellite, where the LNB performs low noise amplification to the received signal; down-converts the signal and transmits this signal to the IDU. The ODU accepts a signal from the IDU, where the transmitter up-converts, amplifies and transmits the signal to the satellite.

Figure 4.3: Indoor Lab Setup.

Figure 4.4: Outdoor Lab Setup.

Table 4.2: Antenna and RF specification.

Item	Parameter	Performance
Antenna	Diameter	1.2 m
	Frequency Range	TX: 14.0 to 14.5 GHz RX: 10.95 to 12.75 GHz
	Gain (middle band) ±0.2 dB	TX: 46.5 dB TX: 45.0 dB
Block Upconverter (BUC)	Output Frequency Range	14.0 to 14.5 GHz
	Input Frequency Range	950 to 1450 MHz
	Output Power (1 dB comp. pt.)	4 watt typical
	Conversion Gain	61 dB typical
	Reference Requirement	10 MHz -5 dBm ± 5 dB
	Operating Temperature Range	-40°C to +55°C
Low Noise Block Downconverter (LNB)	Input Frequency Range	10.7 to 11.7 GHz low band 11.7 to 12.75 GHz high band
	Output Frequency Range	950 to 1950 MHz low band 1100 to 2150 MHz high band
	Conversion gain	50 to 62 dB
	Noise Figure	0.6 dB typical 0.8 dB maximum
	Operating Temperature Range	-30°C to +60°C

4.1.2.2   Visibility Sensor

In cooperation with the environmental protection department in Saudi Aramco, the visibility data for the area of interest namely Dhahran, Saudi Arabia during the last two years has been shared. The sensor used is CS-120 by Campbell Scientific which provides very precise measurements using continuous high-speed sampling, which improves the accuracy of the

measurements taken during mixed weather such as rain and hail, while providing reliable readings during more stable events such as fog and mist. High speed sampling also allows the sensor to better respond to suddenly changing conditions.

Figure 4.5: Visibility sensor in Dhahran station.

4.2 Link Budget

A link budget analysis has been conducted to connect the new VSAT terminal proposed to be used in the test. The improvement in the SNR as well as the system's throughput based on the estimation specific to the region of Dhahran is analysed. The signal to noise power spectral density ratio is presented by:

$$\frac{C}{N_0} = \frac{C}{K.T} = \frac{P_r}{K.T} = \frac{P_t.G_t}{A_t} \cdot \frac{G_r}{K.T} = \frac{EIRP}{A_t} \cdot \frac{G_r}{K.T} \,, \qquad 4.1$$

Where, $\frac{C}{N_0}$ is the carrier to noise ratio

$$\frac{C}{N_0}\Big|_{dB} = 10\log P_t + 10\,logG_t - 10\log A_t + 10\log G_r - 10\log K - 10\log T.$$

$$\frac{C}{N_0}\Big|_{dB} = P_t + G_t - A_t + G_r - K - T \text{ dB.} \qquad 4.2$$

Where A_t (total attenuation) = A_{SD} (DUSA attenuation) + A_0 (free space loss), where A_0 = $(4.\pi.d/\lambda)^2$, d is the distance in *km* between the transmitter (ground station) and receiver (satellite), A_{SD} presents dust and sand attenuations. P_t and P_r are transmitted and received power, and G_t and G_r are antenna gain at transmitter and receiver sides respectively. Also, K represents the Boltzman constant and T represents the effective noise temperature. Assuming a receive filter with noise of equivalent bandwidth (B_r), the noise power (N) will be:

$$N_o.B_r = K.T.B_r \,, \qquad 4.3$$

$$SNR = \frac{C}{N} = \frac{C}{N_0} \cdot \frac{1}{B_r} . \qquad 4.4$$

The symbol energy $E_s = C.T_s = C/R_s$, where the transmission rate R_s and symbol duration T_s = $1/R_s$ hence, energy-to-noise power density per symbol is:

$$SNR = \frac{C}{N_0} \cdot T_s . \qquad 4.5$$

where

$$SNR = \frac{C}{N_0} \cdot \frac{1}{R_s}$$

and in dB:

$$SNR|_{dB} = 10 \, log \frac{C}{N_0} - 10 \log R_s$$

$$\frac{C}{N_0}|_{dB} = P_t + G_t - A_t + G_r - K - T - R_s \quad \text{dB.}$$

4.6

SNR is exploited to find the BER of a digital transmission system. Thermal noise power Spectral density is given by $N_0 = K \cdot T$, where,

K (Boltzman constant) = 1.38 x 10^{-23} Ws/K = -228.6 *dB Ws/K,*

T (Effective noise temperature) = $T_a + T_r$,

T_a (Noise temperature of the Antenna), A_t (Total weather attenuations), and

T_r (Noise temperature of the receiver) = $\left(10^{Nr/10} - 1\right) * 290,$

where noise figure of the LNA, $N_r \approx 0.7$ - 2 dB.

Therefore, QoS is improved by providing enhanced estimates for attenuations due to dust and sand storm that would lead to adjusting SNR output by altering the transmitted power, transmission rate, and gain.

We had analytical and experimental results of SNR and visibility readings.

After the manipulation of raw data we get an experimental attenuation vs visibility plot shown in Figure 4.9.

Using the following attenuation formula for experimental results from [68]:

$$A_t = \frac{P_t G_t G_r}{KTR_s SNR} \quad .$$

4.7

$$A_t(Unit) = \frac{W}{\frac{Ws}{K}.K.\frac{1}{s}} = A_t(Unitless) \quad .$$

4.8

Where,

P_t = W.

G_t = Unit less.

G_r = Unit less.

SNR = Unit less.

K = Ws/K.

T = K.

R_s = 1/s.

Now we used it to evaluate attenuation from SNR values we extracted first. Later, we used analytic expressions from the same study to plot analytic results.

4.2.1   Link Budget Analysis

Although much of Saudi Arabia is dry, there are differences in annual rain attenuation. The region in the North-East near the coast is in ITU Rain Region C, with moderate rain. This is the location of the first gateway earth station (Tanajib). On the other hand, the second earth station is in ITU Rain Region A, with lesser annual rain. Fairly heavy precipitation can occur in the extreme south-west which is in ITU Rain Region E. The rain attenuation values in the table below are based on calculations following the latest issue of ITU prediction method ITU-R P.618.

Table 4.3: Rain attenuation values.

Frequency, GHz	Availability, %	Location and Attenuation in dB		
		Primary Gateway, Tanajib 27.953 N, 48.786 E	Secondary Gateway, Haradh 24.065 N, 49.201 E	Terminal in Central Area 23.88 N, 47.97E
14.25	99.95	2.5	1.2	1.1
	99.90	1.8	0.7	0.7
11.19	99.95	1.5	0.6	0.6
	99.90	1.0	0.4	0.4

The availabilities in Table 4.3 correspond to the annual situation. For the worst-month, the values are not significantly different. For example, in this table the 1.8 dB for 99.9% uplink availability at the primary gateway corresponds to a monthly worst-case availability of 99.6% according to ITU-R publication P.841. The annual values were used for detailed link budgets.

The reasons for selecting the availability percentages shown in the table are:

99.90%:   The basic availability desired by Saudi Aramco.

99.95%:   Used for uplink and downlink fades for the gateway to/from satellite links. The gateway to satellite link must have significantly better availability than the terminal to satellite links so that a fade on the gateway to satellite link will not affect all terminals.

Intelsat 10-02 covers Saudi Arabia with its spot 2 beam. This beam has excellent coverage over the bulk of Saudi Arabia i.e. antenna gain to noise temperature (G/T) = 5 dB excluding the extreme south, but is only 3-4 dB over the entire territory of the kingdom. The "Beam

Edge" specified by Intelsat has a G/T of only 0 dB and covers all of the Middle-East as well as a considerable portion of the Mediterranean and Russia. The data rates that can be supported will very much be dependent on the terminal locations.
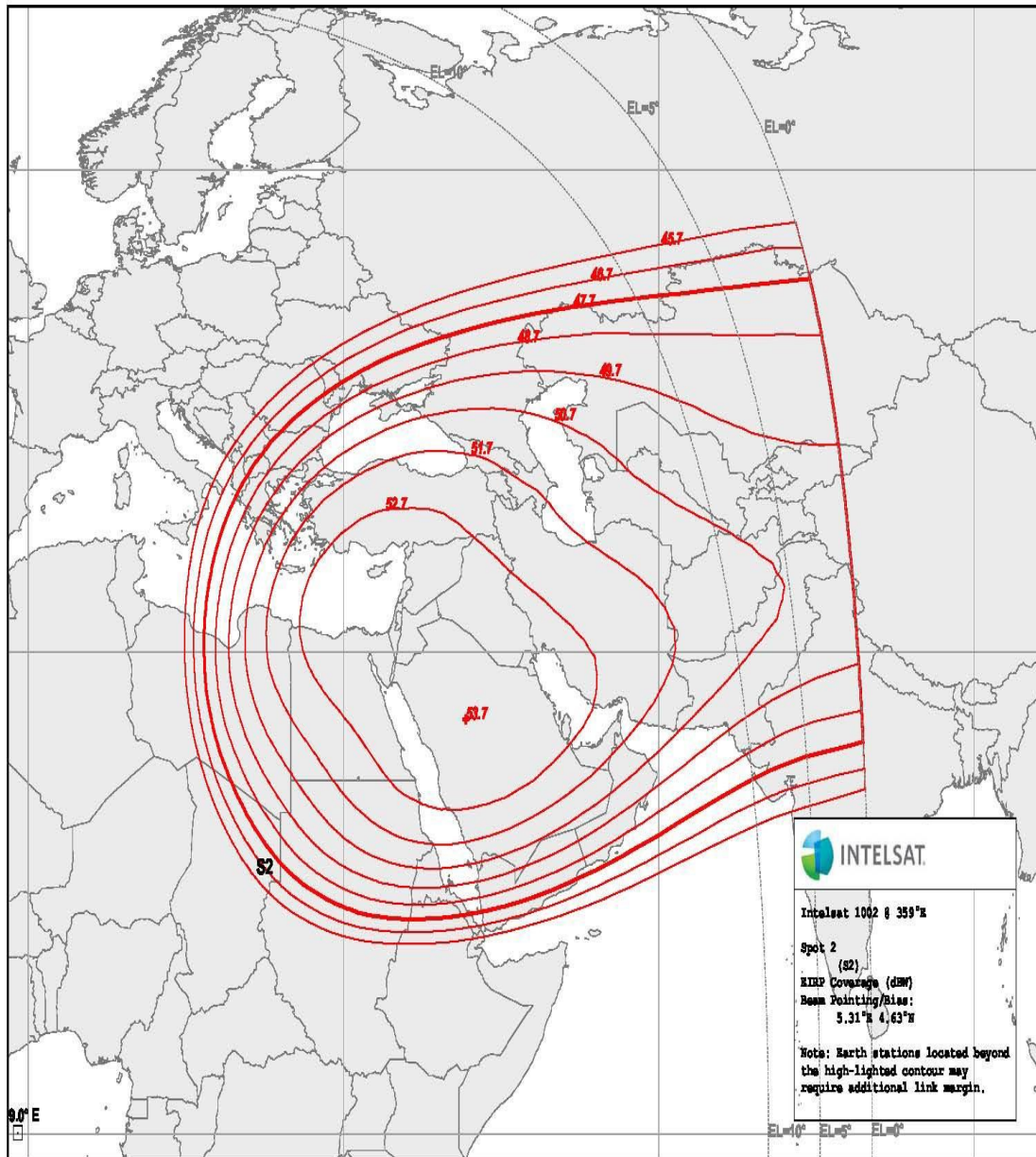
Figure 4.6: Intelsat 1002 beam 2 footprint.

The vast majority of the terminal and gateway locations are in the coverage region that provides 5 dB satellite G/T. However edge locations are limited to only 4 dB G/T.

Satellite data used for the link budgets is summarized in Table 4.4.

Table 4.4: Satellite parameters.

Location	EIRP, dBW	G/T, dB/K	Saturating Flux Density, dBW/m^2
Beam Center	53.7	6	-89.3
Most of Kingdom (including locations of the Gateways)	52.7	5	-88.3
Total Coverage Area defined by Saudi Aramco Example (southern location)	51.7	4	-87.3 (referenced to G/T level)

The values in the table above permit the link availability requirement of 99.9% to be achieved. A summary of link budget results is given below.

4.2.2   Return Link Budget Results

A summary of the return link budget analysis is provided in Figure 4.7 utilizing lease transmission plan (LST5), Intelsat proprietary link budget tool, where details are provided in tables following the summary below. The data applies to a BER of 10^{-7}. The forward error correction coding applied was DVB-RCS Turbo rate 2/3.

INTELSAT.
Closer, by far

Lease Transmission Plan Program (LST)
Lease Summary Information

	SVO-L Number	: 1
IS-1002 at 359.00 °E	Tr. Beam Number	: 75/75
	Slot	: 7-9
	Tr. Cen. Freq. (GHz) :	14.3150 / 11.5150

Note :

Beam Uplink (Geog.)	:	S2	Beam Downlink (Geog.)	:	S2	Tr BW (MHz)	:	112.0
Beam Uplink (Phys.)	:	S2	Beam Downlink (Phys.)	:	S2	Tr BW; (MHz; IESS-410)	:	72.0
Tr. SFD (dBW/m2 ; BP)	:	TBD	Tr. IBO (dB)	:	-6.1	Lease BW usage (MHz)	:	2.4
Tr. SFD (dBW/m2 ; BE)	:	-79.0	Tr. OBO (dB)	:	-4.0	Lease OFD (dBW/m2 ; BE)	:	-99.9
Tr. G/T (dB/K ; BE)	:	.0	Tr. EIRP (dBW ; BE)	:	47.7	Lease EIRP (dBW ; BE)	:	28.9
Tr. G/T (dB/K ; BP)	:	6.5	Tr. EIRP (dBW ; BP)	:	53.7			

Link Analysis Description:

MultiCarrier Txpdr Lease		**Link 1**	
Number of links:	1		
Modulation		QPSK	
Information Rate		2048.0	kbit/s
FEC Code Rate		.6667	
R-S Code Rate		1.0851	
Clear Sky Eb/No Available		7.5	dB
Number of Assigned Carriers		1	
Transmit ES Code		D H	
Transmit ES Size		1.2	m
Receive ES Code		TANAJIB	
Receive ES Size		6.0	m
Receive ES G/T		33.8	dB/K

Total Leased Resource Usage:

LST calculated			Total BW allocated	2.3333	MHz
(MultiCarrier Txpdr Lease)			Total BW PEB	.5270	MHz
Total EIRP utilized	22.3	dBW	Total BW utilized	2.3333	MHz
Total EIRP available	28.9	dBW	Total BW available	2.4000	MHz
Margin (available-utilized)	6.6	dB	Margin (available-utilized)	.0667	MHz

Notes:

Communications Systems Engineering	Data Source: IESS 410. Rev. 8b, May 2001.	v:1.7.2

Carrier Information	Link 1	
Carrier Type	TURBO	
Performance		BER
Modulation	QPSK	
Eb/No Threshold	5.0	dB
C/N Threshold	5.9	dB
Center Frequency	14259.00	MHz
Information Rate (IR)	2048.0	kbit/s
Overhead (OH)	.0	kbit/s
Data Rate (IR + OH)	2048.0	kbit/s
FEC Code Rate	.6667	
R-S Code Rate	204,188	
Transmission Rate	3333.3	kbit/s
Bandwidths and Margins		
Filter Rolloff Factor	.40	
Spreading Factor	1	
Allocated Bandwidth	2.3333	MHz
Noise Bandwidth	1.6666	MHz
Number of Assigned Carriers Per Link	1	
Activity Factor	100.0	%
Total Availability	99.902	%
U/L Availability	99.903	%
D/L Availability	99.998	%
Spec Uplink Rain Margin	N/A	dB
Spec Downlink Degradation Margin	N/A	dB
Computed Uplink Rain Margin	2.50	dB
Computed Downlink Degrad. Margin	11.96	dB
Transmit Earth Station Data		
ES Code	D H	
Intelsat Standard		
Antenna Diameter	1.2	meters
Longitude	50.2	deg. E
Latitude	27.5	deg. N
Elevation Angle	26.0	deg.
Azimuth Angle	249.7	deg.
Pattern Advantage	6.2	dB
Peak Antenna Gain @ operating freq.	43.2	dBi
Sidelobe Constant	32.0	dBi
Sidelobe Gain @ 3 degrees	20.1	dBi
Tracking	None	

Receive Earth Station Data		
ES Code	TANAJIB	
Intelsat Standard		
Antenna Diameter	6.0	meters
G/T of ES at 4 or 11 GHz	33.8	dB/K
Longitude	48.5	deg. E
Latitude	27.5	deg. N
Elevation Angle	27.5	deg.
Azimuth Angle	248.5	deg.
Pattern Advantage	5.7	dB
Peak Antenna Gain @ operating freq.	55.6	dBi
Sidelobe Constant	32.0	dBi
Sidelobe Gain @ 3 degrees	20.1	dBi
Tracking	None	

Per Carrier UL & DL eirp (Clr-Sky)	Link 1	
Transmit ES elevation angle	26.0	deg.
Uplink EIRP per carrier	50.4	dBW
Pathloss at uplink frequency	207.6	dB
Gain of 1 m2 antenna	44.6	dBi
Per carrier FD @SC	-112.7	dBW/m2
SC pattern advantage @ES	6.2	dB
Per carrier BE FD arriving @ SC	-106.5	dBW/m2
Transponder BE SFD	-79.0	dBW/m2
Per carrier input back-off	-27.5	dB
Per carrier output back-off	-25.4	dB
Transponder BE saturation EIRP	47.7	dBW
Downlink BE EIRP	22.3	dBW

LINK BUDGET		
C/N Uplink Per Carrier		
Per carrier uplink EIRP	50.4	dBW
Pathloss at uplink frequency	207.6	dB
Satellite G/T at BE	.0	dB/K
Measured Tpdr G/T Improvement Factor	.0	dB
SC pattern advantage @ES	6.2	dB
C/N uplink, thermal	15.4	dB
C/N ES HPA at ES elevation angle		
HPA IM at 10 degree elevation angle	8.0	dBW/4kHz
C/N ES HPA-IM per carrier at ES elev. angle	22.7	dB
C/I TWTA IM at BE		
Satellite TWTA IM at BE	-16.8	dBW/4kHz
C/I TWTA IM per carrier	13.1	dB
C/N Downlink Per Carrier		
Receive ES elevation angle	27.5	deg.
Per carrier BE EIRP	22.3	dBW
Measured Tpdr DL e.i.r.p. Improv. Factor	.2	dB
SC pattern advantage @ES	5.7	dB
Pathloss at downlink frequency	205.6	dB
ES G/T at tpdr downlink frequency	34.2	dB/K
C/N downlink, thermal	23.2	dB
C/I Co-Channel		
C/I co-channel interference, total	25.2	dB
ASI C/I		
Total Uplink ASI C/I	N/A	dB
Total Downlink ASI C/I	N/A	dB
Total C/N, & Eb/No (clr-sky)		
C/N total per carrier	10.4	dB
Margin for ASI	1.0	dB
Margin for terrestrial losses	.5	dB
Margin for other losses	.6	dB
Margin for HPA - IM (in dB)	.0	dB
C/N total (clear-sky)	8.4	dB
Eb/No total (clear-sky)	7.5	dB

Per Carrier Link Summary	Link 1	
Carrier type	Digital	
Per carrier uplink EIRP	50.4	dBW
Per carrier dnlink EIRP	22.3	dBW
Per carrier total C/N threshold required	5.9	dB
Per carrier total C/N clear sky	8.4	dB
Number of active carriers	1.0	
Total Lease Resource Usage		
Per carrier BE FD arriving @ SC	-106.5	dBW/m2
Total FD @ SC per carrier type	-106.5	dBW/m2
Grand total FD arriving @ SC	-106.5	dBW/m2
Grand total FD (BE) available	-99.9	dBW/m2
Margin (°)	6.6	dB
Per carrier BE EIRP	22.3	dBW
Total BE EIRP per carrier type	22.3	dBW
Grand total EIRP utilized	22.3	dBW
Grand total EIRP available	28.9	dBW
Margin (°)	6.6	dB
Allocated BW per carrier	2.3333	MHz
Total BW per carrier type	2.3333	MHz
Grand total BW allocated	2.3333	MHz
Grand total BW PEB	.5270	MHz
Grand total BW utilized	2.3333	MHz
Grand total BW available	2.4000	MHz
Margin (°)	.0667	MHz

ES Off-Axis EIRP Density Lim.		
Transmit antenna diameter	1.2	meters
Per carrier uplink EIRP	50.4	dBW
Noise BW or EDF	1.6666	MHz
Conversion to per 4 kHz	26.2	dB
Peak antenna gain	43.2	dBi
Power at antenna feed	-19.0	dBW/4kHz
Antenna sidelobe gain @ 3.0 deg	20.1	dBi
Uplink EIRP density @ 3.0 deg	1.0	dBW/4kHz
Off-axis EIRP limit @ 3.0 deg	17.1	dBW/4kHz
Margin (*)	16.0	dB
STD Gx ES On-axis EIRP Lim.		
Per carrier uplink EIRP density	24.2	dBW/4kHz
Gx uplink EIRP density limit	37.0	dBW/4kHz
Margin (*)	12.8	dB
Max. PFD @ Earth's Surface		
Per carrier DL BE EIRP	22.3	dBW
Assumed angle of arrival	5.0	degrees
Pattern adv. @ angle of arrival	4.0	dB
Energy dispersal	1.6666	MHz
Conversion to per 4 kHz	26.2	dB
EIRP density per 4 kHz	.1	dBW/4kHz
Pathloss towards angle of arrival	206.8	dB
Gain of 1 m2 antenna	42.7	dBi
PFD arriving @ earth's surface	-164.0	dBW/m2/4kHz
ITU radio reg. Limit (RR28)	-150.0	dBW/m2/4kHz
Margin (*)	14.0	dB
* Negative margins indicate limits exceeded		

Figure 4.7: Link budget analysis.

61

Table 4.5 shows the results of the link budget analysis conducted for the VSAT remote terminal in Dhahran, Saudi Arabia which shows the antenna and BUC sizes, bit rate, and the fade margin.

Table 4.5: Return link budget results.

Terminal Location	Terminal Type	Terminal Size, Antenna Diameter, m/BUC size, watts	Return Link Bit Rate, kbps	Margin, dB for 99.9% Availability
Dhahran	Fixed	1.2/4	2,048	3.02

4.3   MATLAB Simulation

The attenuation model represented by the observed data has been simulated. The simulations are conducted in MATLAB environment capitalizing on the visibility and SNR values. The results are taken in order to get the BER and QoS thus getting the throughput. The simulation is based on simple topology shown in Figure 4.8.

In this model, the remote terminal is considered to be the one transferring the data to a hub site. Satellite modem encodes and transfers the data received from terminal into digital signals and transmit it to the satellite operating on Ku band. The data is then received at the hub station through the satellite. It is then decoded and actual information is extracted over there. Attenuation factors are introduced, in our case dust and sand models are considered. These factors affect the SNR and BER of the signal. Dust and sand are characterized though visibility. Higher visibility means less dust particles are

suspended in air whereas lower visibility means high amount of sand in air or a sand storm.
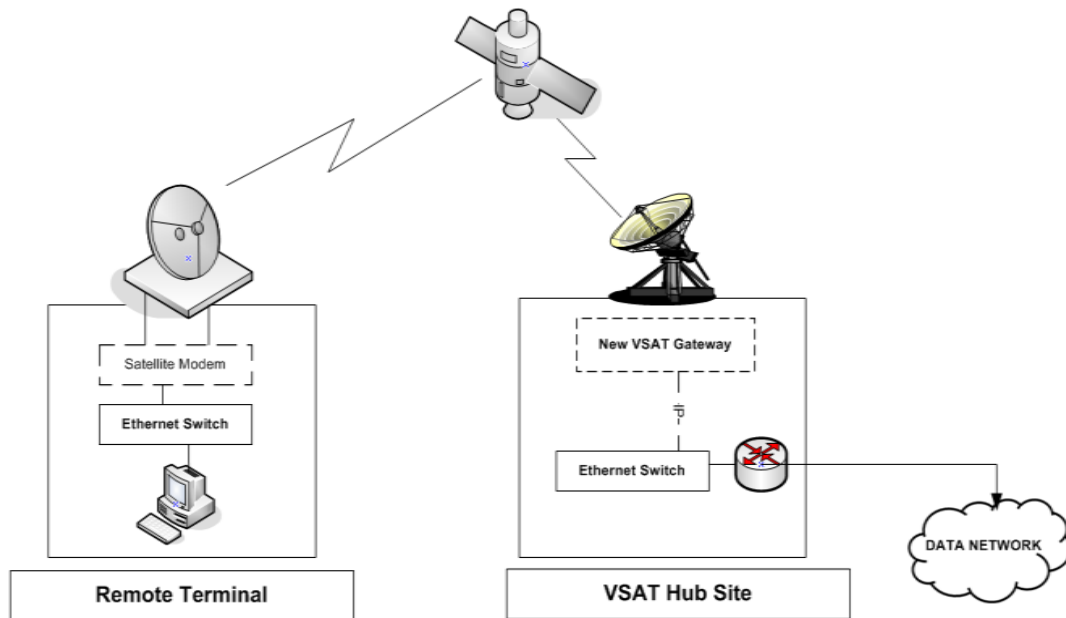
Figure 4.8: System model.

4.3.1 Simulation Methodology

The observed attenuation model along with the other radially available models in the literature were simulated on MATLAB. Our simulation is done on following below steps.

1) Simulation of observed attenuation model.

2) Simulation of applying this model on a Ku-Band DVB-S2 VSAT system.

3) Comparison of observed model with other models in the literature.

4.3.2 Simulation of Observed Attenuation Model

The signal attenuation trend with the visibility recorded throughout the last 2 years in Saudi Aramco VSAT terminal in Dhahran, Saudi Arabia as shown in Appendix I has been simulated after filtering the data according to the dust occurrence focusing on the period from February to July for both years 2012 and 2013. The threshold SNR of the system is 6.5 dB.

The results obtained have been compared with the radially available models in the literature as explained in chapter 3. Specifically, Ahmed et al's DUSA model has been chosen for the comparison. Using the slope/bias scaling fixed point modeling, the attenuation model can be expressed as:

$$A_P(\theta, f) = \rho \times \frac{(5.67 \times 10^4)}{V(\theta) r_{e0}^2 \lambda} \times \frac{\epsilon''}{(\epsilon'+2)^2 + \epsilon''^2} \times \sum_i^n p_i r_i^3 + \delta \ . \qquad 4.9$$

Where,

ρ is the cslope constant

δ is the cbias constant

λ is the wavelength in meters

$V(\theta)$ is the function of visibility in kilometers

ε' and ε'' are the real and imaginary part of the complex dielectric constant of the dust particle

r_{e0} is the radius of the particle in micrometers.

$\sum_i^n p_i r_i^3$ is the dust and sand storm distribution

For round trip:

$$cslope = \rho = 3.5481 \times 10^{-17} (dimension\ less)$$

$$cbias = \delta = 2.2909 \times 10^{-16} (unit\ per\ km)$$

Above expression is the compensated expression of dust and sand model. Two tune parameters are extracted by inspection. By intensive MATLAB tests, it has been figured out that cslope can be integrated back into the original expression by changing $(\epsilon' + 2)^2$ to $(\epsilon' + 9.9595 \times 10^8)^2$. However the cbias have no counter parameter to be modified to compensate it. So, cslope has been used as its numerical value.

Hence the attenuation model after compensation can be expressed as:

$$A_P(\theta, f) = \frac{(5.67 \times 10^2)}{V(\theta)r_{e0}^2 \lambda} \times \frac{\epsilon''}{(\epsilon' + 9.9595 \times 10^8)^2 + \epsilon''^2} \times \sum_i^n p_i r_i^3 + (2.2909 \times 10^{-16}) \quad\quad 4.10$$

The outcome of (4.10) is presented in Figure 4.9 which shows the effectiveness of our model in representing the measured data.
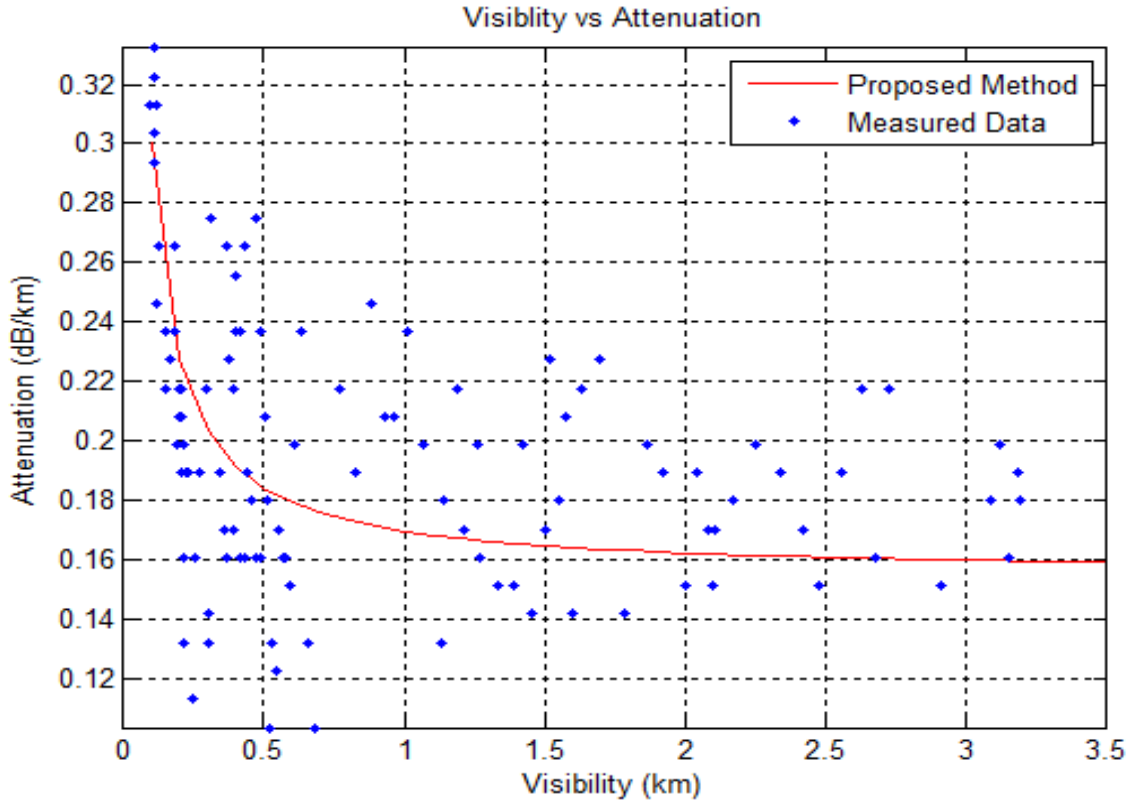
Figure 4.9: Observed compensated dust and sand storms attenuation model.
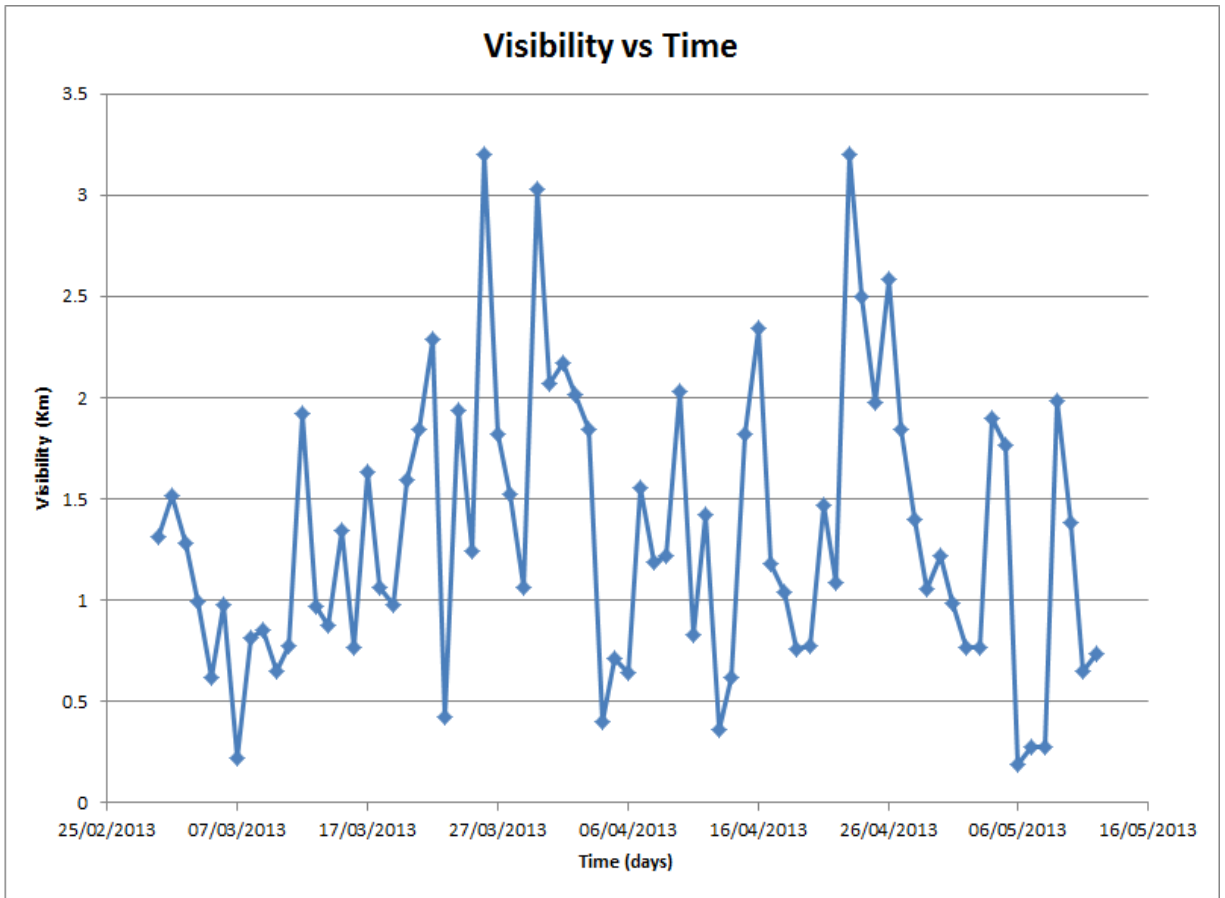
Figure 4.10: Observed visibility data over a sample period of time.

Figure 4.10 shows sample of the visibility data collected from Dhahran station throughout the year of 2013. It is shown that the area encounters severe dust storms during the period from February to May of every year. For example, the visibility can go to few meters as shown in the results sometime in April.

4.3.3   Simulation of DVB-S2 VSAT

Now, we have the attenuation model, there is a need to test this model on a VSAT system. For this purpose, DVB-S2 VSAT is simulated on MATLAB using default DVB-S2 functions provided by communication toolbox. QPSK is used with Turbo code rate of 2/3.
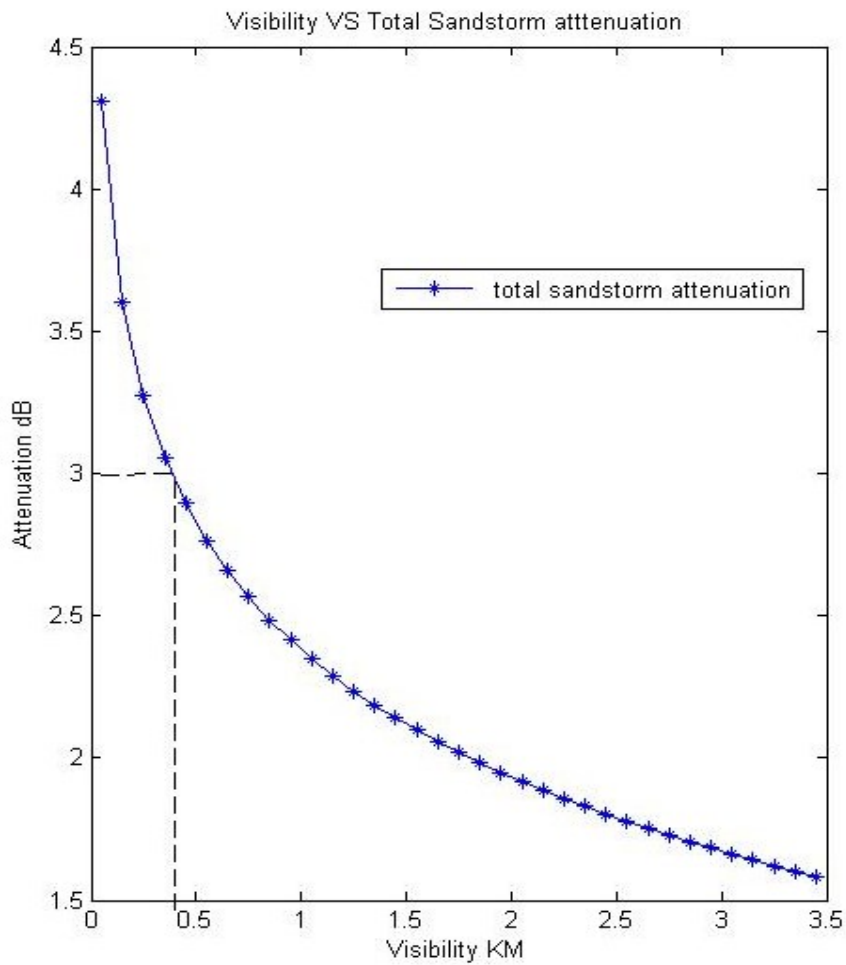
Figure 4.11: Total attenuation trend for observed data.

According to Figure 4.11, earth station experiences up to the maximum of about 4.2 dB in severe sandstorm situation Dhahran, Saudi Arabia in the last 2 years of observation.

67

Also, the system will undergo a link outage if the dust storm is severe with a visibility below 400 *m*.

After the simulation of DVB-S2, attenuation model derived is added into the system in order to compare the performance of the DVB-S2 VSAT system where ACM is enabled in the original scenario and disabled in the other scenario. Figure 4.12 shows the comparison where we can see the performance of the system in both scenarios. In the first scenario, the ACM is fixing the system performance at the threshold. Whereas in the second scenario, the attenuation model effect is clearly shown on the system performance. The attenuation decreases as the visibility increases. At high visibility, the attenuation becomes minimal and the system can maintain the threshold.
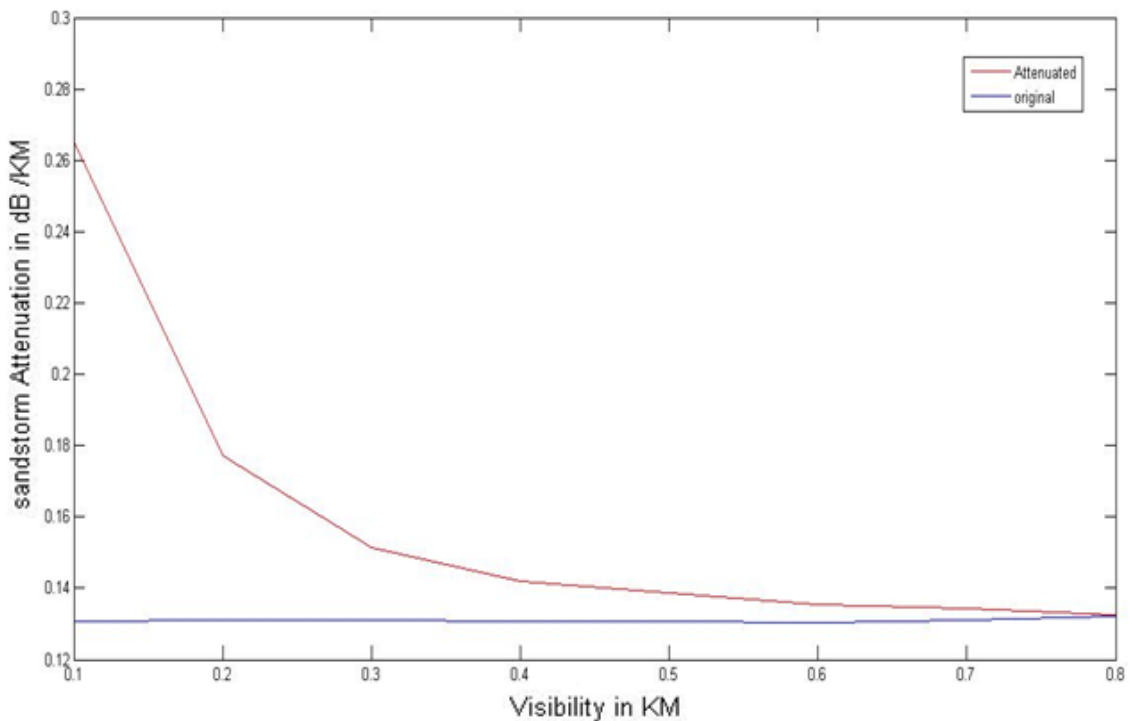
Figure 4.12: DVB-S2 attenuated vs original DVB-S2.

4.3.4   Comparison with other Models

Comparing the developed DUSA model with the other models available in the literature, we found a deviation due to the fact that the study included only the visibility as a variable where other parameters such as particle size, relative permittivity, etc. were not included in the study.
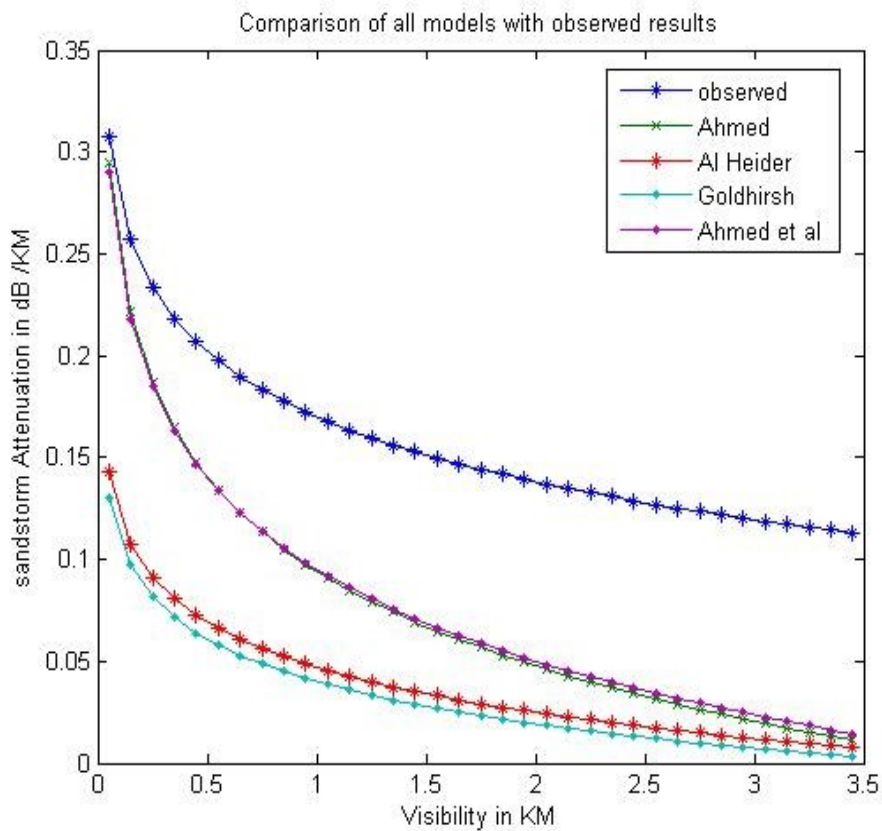
Figure 4.13: Comparison between developed DUSA model with other models.

Figure 4.13 shows a comparison between the observed attenuation model and the other models in the literature which resulted in deviation between the empirical values and theoretical models. There are many possible reasons for the deviation; however, the main

reason is that the attenuation could not be purely caused by dust and sand storms. The attenuation could be caused by other factors including rain, fog, and clouds at the instant signal performance were observed. Nevertheless, at reasonable high visibility above 2 *km* shown in Figure 4.13, the small deviation compared to the fade margin will not affect system performance.

4.4   Mitigation Solutions for the Dust and Sand Storms Attenuation

4.4.1   Link Compensation Techniques Provided by the System

Three measures are available to counteract fading caused by rain fades and dust storm fades, uplink power control for the return (inbound links), uplink power control for the forward (outbound link), and rate reduction for the return links. Uplink power control for the return links operates as follows:

The gateway demodulator estimates the incoming SNR of each terminal and sends the value back to the terminals on the forward link. The terminals compare this value with a (settable) threshold value and increase or decrease their output power so as to maintain the threshold. Since the gateway measures the SNR every 0.848 *sec*., the reaction time is quite sufficient to allow for rapid changes in fade rate.

Once the potential of uplink power control has been exhausted (the terminal's output power is at its maximum but the measured SNR is below the threshold) a rate reduction technique can be used. The terminal drops its symbol rate by a factor of 2 to improve the

SNR. A second drop in symbol rate can also be accommodated. Once the SNR improves upon the cessation of the fade, the terminals revert to the higher rate.

Uplink power control for the forward link is used so that excessive transponder power is not used in the absence of any fade. In the presence of a fade, the gateway's transmit power increases, maintaining a constant flux density at the satellite.

4.4.2   Suggested Mitigation Techniques

1. **Modem level:** An intelligent mechanism to adjust modulation and coding scheme according to the distortion level, in the modem level to mitigate small distortions less than 2 dB.

2. **RF subsystem level:** For a huge distortion greater than 2 dB below the threshold, receiving antenna gain can be increased to mitigate the sandstorm distortion.

4.4.2.1   Auto Coding and Modulation Switching

In this technique, we are proposing using different modulation and coding schemes to counterpart the effects of dust and sand storms on the VSAT system performance degradation.

VSAT Systems use various modulation and coding techniques in practice. Typical modulation schemes used in VSAT systems are namely: FSK, BPSK, QPSK, 8 PSK, QAM, 8 QAM, DPSK, OPSK, MSK, PAM, 16 APSK and 32 APSK. Also, they use coding schemes which are: Convolution, Hamming, Turbo, RS, and LDPC. Below

figures show the result of the simulation for different un-coded and coded modulation schemes run over the developed system.

The wireless channel is then estimated in MATLAB using different modulation and coding schemes that are commonly used in VSAT systems. Below figures and tables depict the results.
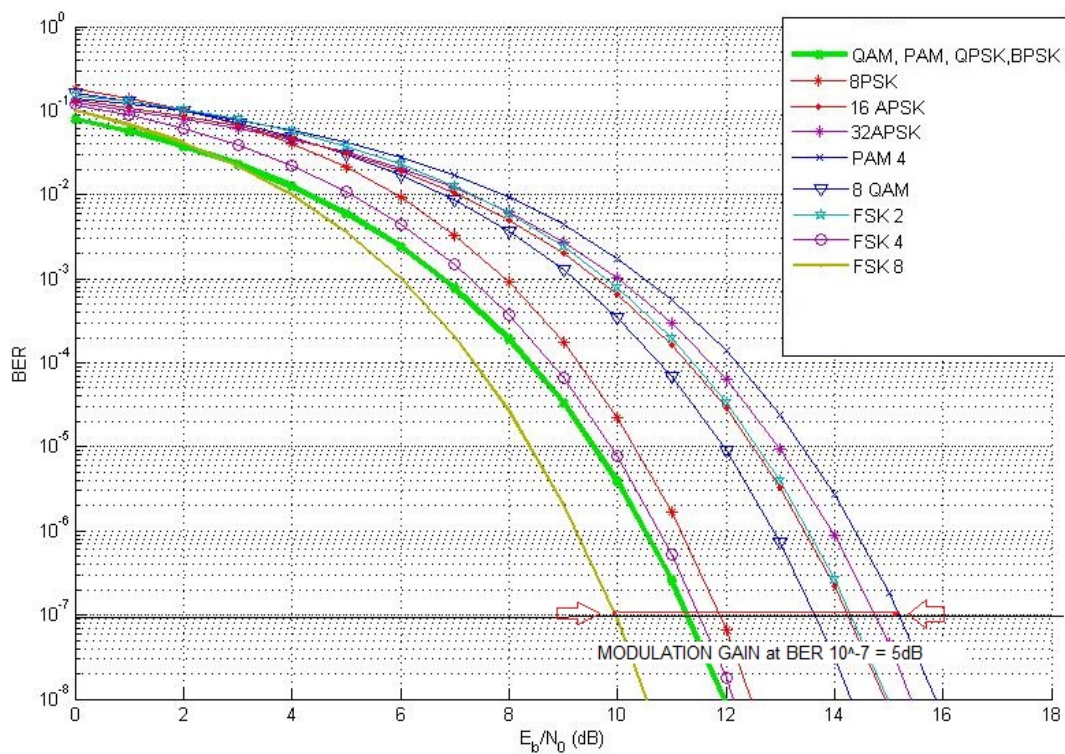
Figure 4.14: Modulation gain comparison between different modulation techniques.

Figure 4.14 shows that among the tested uncoded modulation schemes, best performing modulation scheme was FSK 8 while PAM 4 was the lease performing scheme. Modulation scheme switching between PAM 4 to FSK 8 can obtain about 5.2 dB as shown in Figure 4.14. BPSK, QPSK, QAM, PAM are overlapped in the same line and show the similar performance. When switching the modulation scheme from BPSK,

QPSK, QAM, PAM to 8FSK can obtain nearly 1.2 dB gain. For a system designed for threshold BER of 10^{-7}, it needs a minimum of 10 dB E_b/N_0, while other modulation schemes require higher threshold.
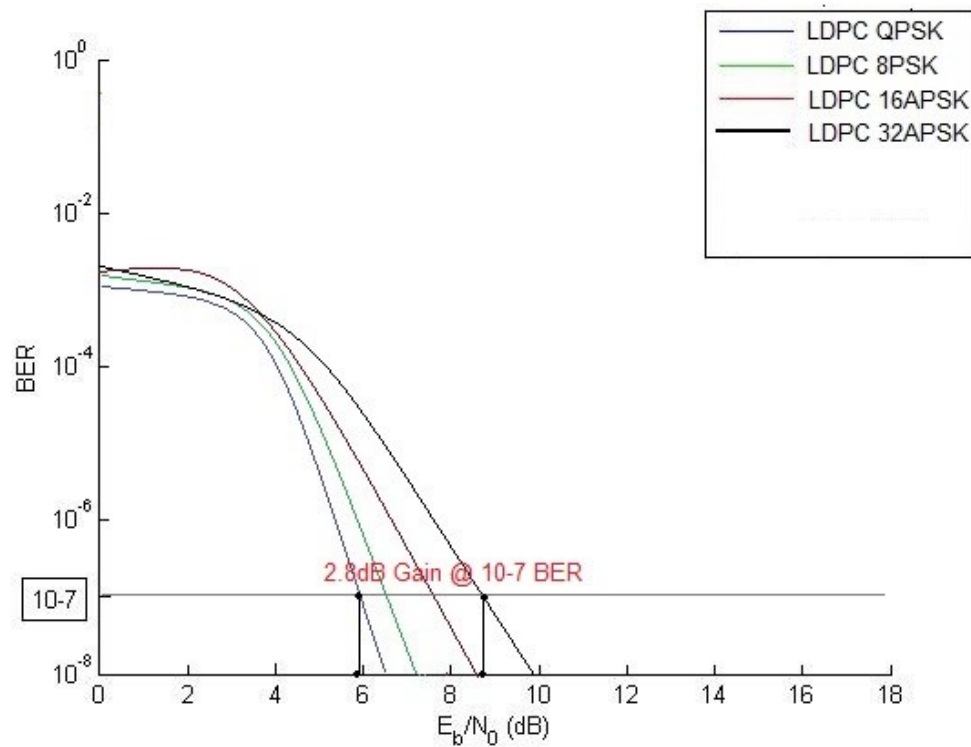
Figure 4.15: Comparison of LDPC coded modulation schemes.

According to Figure 4.15, if the coding scheme switched from LDPC 32APSK to LDPC QPSK, the system can gain about 2.8 dB margin in order to achieve BER 10^{-7}. Also, the gain can be measured between other coding schemes.

Minimum threshold to meet BER of 10^{-7}:

LDPC QPSK: 5.9 dB

LDPC 8PSK: 6.5 dB

LDPC 16APSK : 7.8 dB

LDPC 32APSK: 8.7 dB

So, LDPC QPSK can be used for poor weather conditions comparatively.
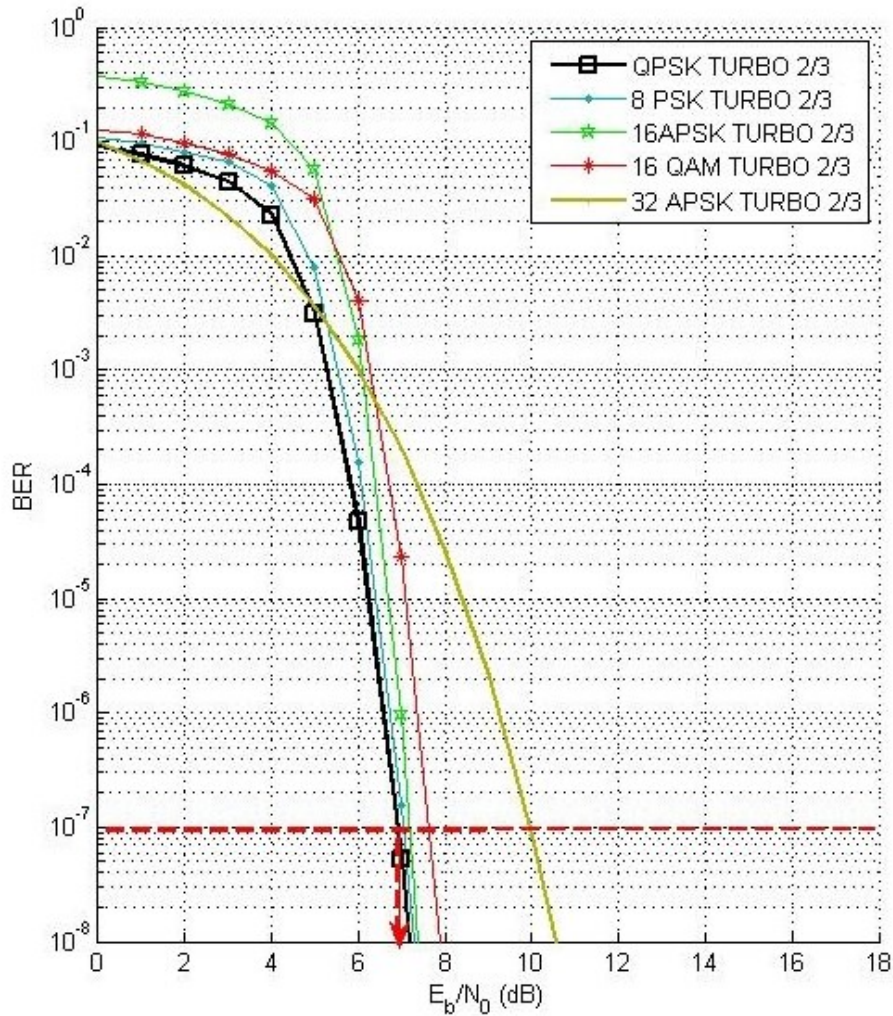
Figure 4.16: Comparison of Turbo coded modulation schemes.

Figure 4.16 shows that switching from LDPC 8PSK to LDPC QPSK can gain nearly 1 dB (as shown in the red arrows) at BER 10^{-7}. Also, switching from QPSK turbo to QPSK

LDPC will gain 1 dB gain. For a system with minimum threshold is 7 dB can be switched

to QPSK LDPC and reduce the threshold to 5.9 dB.

Table 4.6: BER vs E_b/N_0 for different modulation schemes, MATLAB simulated theoretical comparison.

Modulation scheme New	Required E_b/N_0 threshold for BER 10^{-7} in dB	Modulation scheme used earlier and Gain achievable by Switching to new modulation												
		8FSK	QAM	BPSK	QPSK	PAM	4FSK	2FSK	4DPSK	DPSK	OQPSK	8QAM	8PSK	4QAM
8FSK	10	0	1.4	1.4	1.4	1.4	1.6	1.9	3.6	4.2	4.2	4.4	4.8	5.2
QAM	11.4	-1.4	0	0	0	0	0.2	0.5	2.2	2.8	2.8	3	3.4	3.8
BPSK	11.4	-1.4	0	0	0	0	0.2	0.5	2.2	2.8	2.8	3	3.4	3.8
QPSK	11.4	-1.4	0	0	0	0	0.2	0.5	2.2	2.8	2.8	3	3.4	3.8
PAM	11.4	-1.4	0	0	0	0	0.2	0.5	2.2	2.8	2.8	3	3.4	3.8
4 FSK	11.6	-1.6	-0.2	-0.2	-0.2	-0.2	0	0.3	2	2.6	2.6	2.8	3.2	3.6
2 FSK	11.9	-1.9	-0.5	-0.5	-0.5	-0.5	-0.3	0	1.7	2.3	2.3	2.5	2.9	3.3
4 DPSK	13.6	-3.6	-2.2	-2.2	-2.2	-2.2	-2	-1.7	0	0.6	0.6	0.8	1.2	1.6
DPSK	14.2	-4.2	-2.8	-2.8	-2.8	-2.8	-2.6	-2.3	-0.6	0	0	0.2	0.6	1
OQPSK	14.2	-4.2	-2.8	-2.8	-2.8	-2.8	-2.6	-2.3	-0.6	0	0	0.2	0.6	1
8 QAM	14.4	-4.4	-3	-3	-3	-3	-2.8	-2.5	-0.8	-0.2	-0.2	0	0.4	0.8
8 PSK	14.8	-4.8	-3.4	-3.4	-3.4	-3.4	-3.2	-2.9	-1.2	-0.6	-0.6	-0.4	0	0.4
4 PAM	15.2	-5.2	-3.8	-3.8	-3.8	-3.8	-3.6	-3.3	-1.6	-1	-1	-0.8	-0.4	0

Based on Table 4.6, below results have been derived:

- The best uncoded modulation scheme workable for BER: 10^{-7} would be 8FSK with E_b/N_0 threshold of 10 dB.

- The best modulation switching gain could work in between 4QAM to 8FSK. 5.2

  dB could be obtained by switching the modulation from 4QAM to 8FSK. In this

  case link rate also will be doubled.

- The minimum gain could be obtained at uncoded QAM / BPSK / QPSK / PAM to

  uncoded 8FSK. The gain is worth 1.4 dB that can be achieved by switching the

  modulation scheme to uncoded 8FSK.

Table 4.7: Comparison using different code rates.

Coding scheme switch to	Required E_b/N_0 threshold for BER 10^{-7} in dB	BPSK Rs 2/3	BPSK RS 2/3 Diff	BPSK CONV	BPSK RS 8/9	BPSK GOLAY	BPSK RS 1/2	BPSK Hamming
BPSK RS 2/3	6.8	0	0.7	0.8	1.3	2.3	3.7	3.8
BPSK RS 2/3 Differential	7.5	-0.7	0	0.1	0.6	1.6	3	3.1
BPSK Convolution	7.6	-0.8	-0.1	0	0.5	1.5	2.9	3
BPSK RS 8/9	8.1	-1.3	-0.6	-0.5	0	1	2.4	2.5
BPSK Golay	9.1	-2.3	-1.6	-1.5	-1	0	1.4	1.5
BPSK RS ½	10.5	-3.7	-3	-2.9	-2.4	-1.4	0	0.1
BPSK Hamming	10.6	-3.8	-3.1	-3	-2.5	-1.5	-0.1	0

Based on Table 4.7, below results have been derived:

- For an earth station working on BPSK modulation, it can switch to different

  coding schemes in the sandstorm or other attenuation instances to obtain further

  coding gain and mitigation of the additional attenuation. Hence, the system can

  avoid link outage.

- In such case, BPSK Reed Solomon 2/3 works better in the performance; which

  requires only 7 dB threshold E_b/N_0.

- The best coding gain achievable by switching the coding scheme from Hamming to RS 2/3 which could provide about 3.8 dB additional coding gain.

- Depending on the current coding scheme and the attenuation level, coding scheme can be switched to next.

Table 4.8: Comparison using QPSK.

Coding scheme switch to	Required E_b/N_0 threshold for BER 10^{-7} in dB	QPSK Uncoded	QPSK Convolution Hard	QPSK RS 8/9	QPSK RS 2/3	QPSK RS ½
QPSK Uncoded	11	0	-3.2	-2.9	-4.1	-4
QPSK Convolution Hard	7.8	3.2	0	0.3	-0.9	-0.8
QPSK RS 8/9	8.1	2.9	-0.3	0	-1.2	-1.1
QPSK RS 2/3	6.9	4.1	0.9	1.2	0	0.1
QPSK RS ½	7	4	0.8	1.1	-0.1	0

Based on Table 4.8, below results have been derived:

- The best coding scheme suitable for a noisy QPSK channel would be RS 2/3 , which requires 6.9 dB minimum E_b/N_0 as the threshold.

- The maximum additional coding gain can be achieved, when a QPSK RS 8/9 system is switched to QPSK RS 2/3, it can gain up to 1.2 dB.

Table 4.9: Comparison of 8FSK with different code rates.

Coding scheme switch to	Required E_b/N_0 threshold for BER 10^{-7} in dB	8FSK RS 2/3	8FSK RS 1/2	8FSK RS 8/9	8FSK UNCODE	4FSK RS 2/3	2FSK uncoded	8FSK CONV
8FSK RS 2/3	7.2	0	0.4	0.7	1.4	1.6	3.4	7.1
8FSK RS ½	7.6	-0.4	0	0.3	1	1.2	3	6.7
8FSK RS 8/9	7.9	-0.7	-0.3	0	0.7	0.9	2.7	6.4

8FSK UNCODE	8.6	-1.4	-1	-0.7	0	0.2	2	5.7
4FSK RS 2/3	8.8	-1.6	-1.2	-0.9	-0.2	0	1.8	5.5
2FSK uncoded	10.6	-3.4	-3	-2.7	-2	-1.8	0	3.7
8FSK CONV	14.3	-7.1	-6.7	-6.4	-5.7	-5.5	-3.7	0

Based on Table 4.9, below results have been derived:

- The highest performing code in the FSK noisy channel is 8FSK RS 2/3 with the minimum threshold E_b/N_0 of 7.2 dB for BER of 10^{-7}.

4.4.2.2   Adaptive Antenna Sizing

The final SNR of the receiving earth station depends on antenna gain as well, which can be observed in the link budget calculation.

Hence, SNR is directly proportional to the receiving antenna gain. Antenna gain adjustment causes the SNR change in the system. If the antenna gain increased, then the SNR will be increased accordingly.

Based on the parabolic antenna gain equation, antenna gain depends on the diameter of the antenna as specified by (2.4).

The simulation work was performed to check the antenna size adjustment mechanism in MATLAB environment to verify whether SNR can be improved by adjusting the antenna diameter. Simulation coding comprises of link budget and parabolic antenna equations.

Table 4.10: SNR comparison after adjustment.

SNR Reading During Sandstorm (dB)	Antenna Gain (dB)	Antenna diameter (*m*)	Adjusted New Antenna Diameter (*m*)	New Antenna Gain (dB)	New SNR Reading after size adjustment (dB)
6.5	55.8	6	6	55.8	6.5
6	55.8	6	6.35	56.3	6.5
5.5	55.8	6	6.75	56.8	6.5
5	55.8	6	7.15	57.3	6.5

The required threshold SNR of 6.5 dB corresponds to an antenna diameter of 6 *m*. Thus, the results show that, system SNR can be restored by adjusting the antenna size. For example, if the SNR reading is 5 dB which is 1.5 dB below the threshold, if the antenna size increases to 7.15 *m* there will be a gain of 1.5 dB which compensate for the signal performance degradation and hence maintain the link availability. This mechanism could be adopted for SNR distortion of more than 2 dB. Since small distortions can be mitigated by coding and modulation adjustments. Otherwise, this can be applied to DVB-RCS system, which uses ACM scheme. This system has the best coding scheme technically with the highest coding gain.

So, when a DVB-S2 system fails, it doesn't have further room for coding adjustment to mitigate the loss. Therefore, the only option left would be adjusting the antenna.
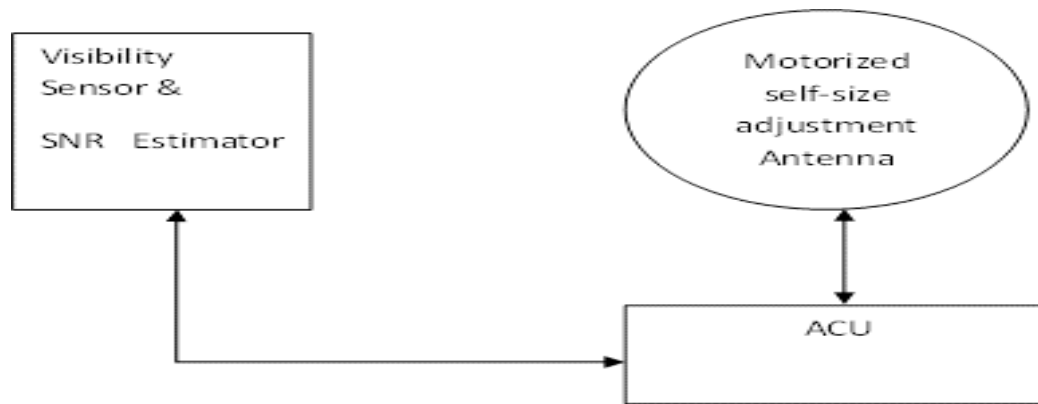
Figure 4.17: System architecture for a self-size adjustment antenna sub-system.

Figure 4.17 shows the block diagram of the suggested adaptive size antenna which consists of a visibility sensor along with an SNR estimator and a motorized antenna controlled by an automatic control unit (ACU). The visibility sensor and the SNR estimator adopts our proposed DUSA model in which sends a feedback signal to the ACU to change the antenna size based on the severity of the dust and sand storms.

CHAPTER 5

CONCLUSION AND FUTURE WORKS

5.1   Introduction

Chapter 5 provides summary, conclusions and recommended future work that can be done as an extension to this work.

5.2   Summary and Conclusions

An ongoing effort in one of the most crucial enabling broadband technologies namely VSAT test beds is the evaluation of the effects of different metrological parameters on the system reliability and performance. This research is established to answer the open question of how severe is the effect of dust and sand storms on satellite communication systems.

In chapter 2, we studied the major metrological parameters that might be of a degradation source for satellite communication systems in the area under investigation namely Dhahran, Saudi Arabia. These parameters include dust and sand storms, foliage, and rain.

In chapter 3, we studied the radially available dust and sand attenuation models in literature and suggested a methodology for estimating dust and sand attenuations based on physical measurements.

In chapter 4, experimental work and numerical results were presented and analyzed. In the practical experiment, we observed the signal performance along with one of the metrological parameters namely visibility over the past two years. An attenuation model for dust and sand storms has been estimated based on the collected data. The model then has been simulated on a DVB-S2 VSAT system. The work showed good matching results between field measurements and simulation results. Results shown that the earth station experienced up to a maximum of more than 4.2 dB attenuation, throughout the last two years, in severe sandstorm situation in Dhahran, Saudi Arabia. In addition, when the system's SNR went below the threshold, system experienced a link outage of 252 minutes more than the designed value. So, dust and sand storms attenuation becomes more severe than the expected in the recent years in the kingdom. Most of the theoretical models were compared and analyzed against the observed model and showed a deviation between the empirical values and theoretical models. There are many possible reasons for the deviation; however, the main reason is that the attenuation could not be purely caused by dust and sand storms. The attenuation could be caused by other factors including rain, fog, and clouds at the instant signal performance were observed. Yet, the minor deviation at high visibility between the existing and proposed models can be mitigated.

As mitigation for the above mentioned degradation on the system performance, two solutions techniques have been studied to compensate for the attenuation. First technique suggests adjusting the antenna gain and the other suggests switching to the best modulation and coding combination to obtain additional gain.

First option is very innovative to be exploited when the weather is very harsh uplink power control mechanism is no longer a valid option. This technique is more effective and simple to increase the SNR and restore to at least its threshold. Antenna again adjustment needs only diameter changes with the coordination of ACU and beacon receiver. However, it could be a special design concept where feed focus point has to change according to the size. Latest VSAT systems use DVB-S2 protocol with LDPC coding which could work for very less SNR like 6.5 dB. However, when the LDPC based systems face link outages, coding gain mechanism would not be workable here. Therefore, the only option left is to adjust the antenna size. Antenna sizes are decided in the design stages with an optimized cost benefits and link budget calculations. Link budget influenced by the rain, sand and storms attenuation. In case of severe weather changes and huge rain or dust and sand storms, the actual attenuation exceeds the predicted value, so it affects the link and SNR accordingly. Therefore, in such situation antenna size change can be an effective solution for the mitigation.

For a reasonable loss like attenuation less than 2 dB, the second technique which suggests altering the modulation or coding schemes to obtain an additional gain at the modem level. Since not all VSAT systems are designed for LDPC, some systems operating with convolution, turbo, or RS can mitigate the attenuation through this technique. Hence, the system can sustain the minimum E_b/N_0 for the required BER.

The research leads to a hardware controller which is continuously monitoring the SNR and BER of the received signal. It has uplink power control, adaptive antenna sizing, and

can change the modulation and coding schemes. This controller will be able to decide the uplink power and scheme based on the atmosphere conditions.

Figure 5.1 shows the block diagram of the controller. It can be seen that the proposed controller is based on constant feedback model. The AAS, UPC and ACM will be adjusted according to the feedback by the system. The hardware controller will ensure the smooth communications under dusty environment. Since it is an additional hardware to the system which is continuously monitoring the SNR and BER and controlling the power, antenna size, and modulation scheme, this will add a delay and will be requiring sufficient resources to work.
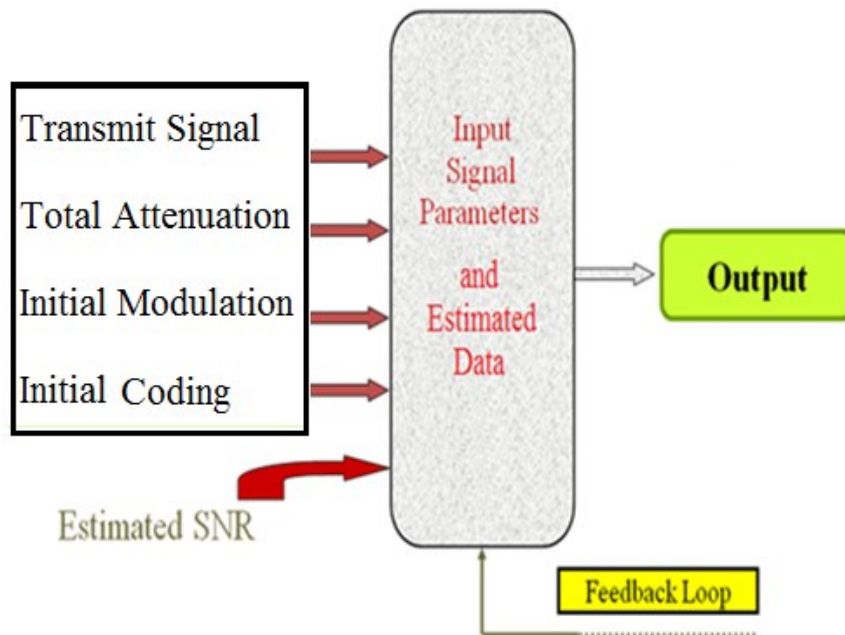
Figure 5.1: Proposed Controller.

5.3   Recommended Future Work

- In the field measurements, visibility was the only parameter that was captured throughout the course of the testing due to the limitation of the test setup. In such studies, all parameters including frequency, particle size, and relative permittivity, storm height, path length, polarization changes during dust and stand storm can to be considered in order to further validate the results. Also, the attenuation was assumed to be originated by dust and sand storms. However, in reality, attenuation can be caused by different factors including rain, cloud, fog, scintillation and other factors during the dust and sand storms time. Hence, these reasons can overestimate the dust and sand storms attenuation value. So, the future research needs a careful observation of all impairments at the same time.

- The VSAT system considered was a Ku band based which is less prone to weather condition changes compared to a Ka band based VSAT system. These systems are the trend in the broadband sector. So, it's recommended as future work to consider conducting a similar test on a Ka band VSAT system to quantify the dust and sand storms effects on the link performance.

- Future research demands more sophisticated design of the proposed intelligent size changing parabolic antenna considering its mechanical design.

APPENDIX

Values of Measured SNR under Different Visibilities.

Day/Time	Visibility	SNR
	(*Km*)	(*dB*)
03-03-13/00:00	0.0963	7.2500
03-03-13/00:10	0.1054	7.0500
03-03-13/00:20	0.1103	7.5000
03-03-13/00:30	0.1200	7.3000
03-03-13/00:40	0.1496	8.2500
03-03-13/00:50	0.1641	8.2000
03-03-13/01:00	0.1783	8.1500
03-03-13/01:10	0.1802	7.8000
03-03-13/01:20	0.1969	8.3500
03-03-13/01:30	0.2027	8.6500
03-03-13/01:40	0.2306	8.4000
03-03-13/01:50	0.2400	8.5500
03-03-13/01:00	0.2752	8.8500
03-03-13/02:10	0.2874	8.5000
03-03-13/02:20	0.3061	8.4750

03-03-13/02:30	0.3185	8.3091
03-03-13/02:40	0.3222	8.5000
03-03-13/02:50	0.3401	8.6500
03-03-13/03:00	0.3593	8.1500
03-03-13/03:10	0.3628	8.7500
03-03-13/03:20	0.3704	8.6000
03-03-13/03:30	0.3841	8.5000
03-03-13/03:40	0.3995	8.7500
03-03-13/03:50	0.4082	8.2000
03-03-13/04:00	0.4178	8.1000
03-03-13/04:10	0.4208	8.6258
03-03-13/04:20	0.4367	8.6000
03-03-13/04:30	0.4580	8.7000
03-03-13/04:40	0.4695	8.9000
03-03-13/04:50	0.4878	8.8500
03-03-13/06:00	0.5093	8.7000
03-03-13/06:10	0.5272	9.0159
03-03-13/06:20	0.5300	8.6000
03-03-13/06:30	0.5464	8.9500
03-03-13/06:40	0.5597	9.0455

03-03-13/06:50	0.5758	9.7250
03-03-13/07:00	0.5859	8.5000
03-03-13/07:10	0.5952	8.9500
03-03-13/07:20	0.6098	7.9091
03-03-13/07:30	0.6289	8.0000
03-03-13/07:40	0.6329	6.5000
03-03-13/07:50	0.6424	9.2250
03-03-13/08:00	0.6637	8.6500
03-03-13/08:10	0.6881	8.7045
03-03-13/08:20	0.7042	8.0000
03-03-13/08:30	0.7282	8.4750
03-03-13/08:40	0.7426	8.8333
03-03-13/08:50	0.7595	7.0000
03-03-13/09:00	0.7752	9.0000
03-03-13/09:10	0.8000	8.9500
03-03-13/09:20	0.8571	8.3591
03-03-13/09:30	0.9091	7.5000
03-03-13/09:40	0.9346	8.2432
03-03-13/09:50	0.9677	8.4375
03-03-13/10:00	1.0000	7.9500

03-03-13/10:10	1.0526	8.9530
03-03-13/10:20	1.1029	8.4000
03-03-13/10:30	1.1628	8.5750
03-03-13/10:40	1.2000	8.7112
03-03-13/11:50	1.2605	8.5000
03-03-13/11:00	1.3043	7.0833
03-03-13/11:10	1.3699	8.7375
03-03-13/11:20	1.4085	8.7545
03-03-13/11:30	1.4563	9.1167
03-03-13/11:40	1.5000	8.8301
03-03-13/11:50	1.5625	8.7264
03-03-13/12:00	1.6043	9.0585
03-03-13/12:10	1.6760	7.9773
03-03-13/12:20	1.7045	8.5784
03-03-13/12:30	1.7857	9.1222
03-03-13/12:40	1.7964	7.8511
03-03-13/12:50	1.8072	6.7009
03-03-13/13:00	1.8182	8.9765
03-03-13/13:10	1.8293	9.1273
03-03-13/13:20	1.8405	9.1091

03-03-13/13:30	1.8519	8.9750
03-03-13/13:40	1.8634	8.5400
03-03-13/13:50	1.8868	8.8709
03-03-13/14:00	1.9108	7.6937
03-03-13/14:10	1.9231	8.6333
03-03-13/14:20	1.9355	8.7312
03-03-13/14:30	1.9481	8.6251
03-03-13/14:40	1.9608	8.6941
03-03-13/15:50	1.9737	8.9045
03-03-13/16:00	1.9868	8.7136
03-03-13/16:10	2.0000	8.9917
03-03-13/16:20	2.0134	8.4400
03-03-13/16:30	2.0270	8.8618
03-03-13/16:40	2.0408	8.5778
03-03-13/16:50	2.0548	8.7430
03-03-13/17:00	2.0690	8.6514
03-03-13/17:10	2.0833	8.7994
03-03-13/17:20	2.0979	8.9538
03-03-13/17:30	2.1583	8.8125
03-03-13/17:40	2.2059	8.7495

03-03-13/17:50	2.2556	8.5028
03-03-13/18:00	2.3077	8.4643
03-03-13/18:10	2.3810	8.6659
03-03-13/18:20	2.4000	8.8023
03-03-13/18:30	2.4590	9.0200
03-03-13/18:40	2.5000	8.8239
03-03-13/18:50	2.5641	8.6250
03-03-13/19:00	2.6087	8.7250
03-03-13/19:10	2.6316	8.2700
03-03-13/19:20	2.6549	8.8279
03-03-13/19:30	2.6786	8.9000
03-03-13/19:40	2.7027	8.5563
03-03-13/19:50	2.7273	8.2784
03-03-13/20:00	2.7523	8.4030
03-03-13/20:10	2.7778	8.6132
03-03-13/20:20	2.8037	8.5000
03-03-13/20:30	2.8302	8.8153
03-03-13/20:40	2.8571	8.6750
03-03-13/20:50	2.8846	8.6347
03-03-13/21:00	2.9126	8.9700

03-03-13/21:10	2.9412	8.5932
03-03-13/21:20	2.9703	8.9065
03-03-13/21:30	3.0000	8.6217
03-03-13/21:40	3.0303	8.8875
03-03-13/21:50	3.0612	8.9277
03-03-13/22:00	3.0928	8.6864
03-03-13/22:10	3.1250	8.5220
03-03-13/22:20	3.1579	8.9182
03-03-13/22:30	3.1915	8.6194
03-03-13/22:40	3.2000	8.7289

REFERENCES

[1]   Satellite Networks, "Electronic Communications Committee (ECC) Report 152, within the European Conference of Postal and Telecommunications Administrations (CEPT) THE USE OF THE FREQUENCY BANDS 27.5-30.0 GHz AND 17.3-20.2 GHz", Gothenburg, Sept., 2010.

[2]   G. Maral, VSAT Networks. West Sussex, England: Wiley, 2004.

[3]   E.M. Saleh I.M. Abuhdima, "Effect of sand and dust storms on microwavepropagation signals in southern Libya", 15th IEEE Mediterranean Electrotechnical Conference, pp. 695 − 698, 2010.

[4]   Huang, W. Rafferty, M. Sue P. Estabrook, "A 20/30 GHz personal access satellite system design", ICC, Boston, MA, pp. 216–222, 1989.

[5]   E. Laborde, A. Stermn, P. Sohn L. Palmer, "A personal communication network using a Ka-band satellite", vol. 10, pp. 401–417, 1992.

[6]   T. A. Russel L. J. Ippolito, "Propagation considerations for emerging satellite communication applications", vol. 81, pp. 923–92, 1993.

[7]   F. Davarian, "Earth-satellite propagation research", vol. 32, pp. 74–79, 1994.

[8]   B. G. Evans M. J. Willis, "Fade countermeasures at Ka band for OLYMPUS", vol. 6, pp. 301–311, 1988.

[9]   B. K. Levitt, "Rain compensation algorithm for ACTS mobile terminal", vol. 10, pp. 358–363, 1992.

[10]   E. Vilar M. Filip, "Optimum utilization of the channel capacity of a satellite link in the presence of amplitude scintillations and rain attenuation", Int. J. Satell. Commun, vol. 38, pp. 1958–1965, 1990.

[11]   E. Vilar M. Filip "Adaptive modulations as a fade countermeasure: An OLYMPUS experiment", Int. J. Satell. Communication , vol. 8, pp. 31–41, 1990.

[12]   J. Horle, "Up-link power control of satellite earth-stations as a fade countermeasure of 20/30 GHz communications systems", International Journal of Satellite Communications (ISSN 0737-2884), vol. 6, July-Sept. 1988, p. 323-330.

[13]   R. E. Peile E. R. Berlekamp, "The application of error control to communications", vol. 25, pp. 44–57, 1987.

 [14]   D. W. Blood R. K. Crane, Handbook for the estimation of microwave propagation effects-Links calculations for earth-space paths (path loss and noise estimation): NASA Goddard Space Flight Center, Greenbelt, MD, Tech, 1979.

[15]   Ying-Le Li, Jia-dong Xu,Hui Zhang and Ming-jun Wang Qun-feng Dong, "Effect of Sand and Dust Storms on Microwave Propagation", vol. 1, PP 1-7, 2013.

[16]   J. Vivekanandan, J Geophy Res D F. S. Solheim, "Propagation delays induced in GPS signals by dry air, water, vapor, hydrometeors and other particulates", vol. 104, pp. 9663-9670, 1999.

[17]   R. E. Hushcke, Ed., Glossary of Meteorology. Boston, MA: Amer. Meteorological Soc., 1995.

[18]   Sami M. Sharief Samir I. Ghobrial, "Microwave Attenuation and Cross Polarization in Dust Storms", vol. ap-35, no.4, April 1987.

[19]   R. A. Bagnold, The Physics of Blown Sand and Desert Dunes. London, U.K.: Chapman & Hall, 1984. First published in 1941.

[20]   S.I., Ali, I.A., Hussien, H.M Ghobrial, "Microwave attenuation in sand storms", Int. Symp. on Antenna and Propagation, Sendai, Japan, 1978.

[21]   "Bangnold, R.A.: The physics of blown sand and desert dunes", 1973.

[22]   T.S. chu, "Effect of sand storms on microwave propagation", vol. 58, Bell Syst.Tech.J, pp. 549-555, 1978.

[23]   A.Ali, M.A.Alhaider A.S.Ahmed, "Airborne dust size analysis for tropospheric propagation of millimetric waves into dust storms", vol. 25, pp. 599-693, 1987.

[24]   A. A. Ali, "Effect of particle size distribution on millimeter wave propagation into sandstorms", vol. 6, pp. 857–868, 1986.

[25]   M. R. Islam, A. Z. Alam, A. F. Ismail, K. Al-Khateeb and Z. Elabdin E. A. A. Elsheikh, "The Effect of Particle Size Distributions on Dust Storm Attenuation Prediction for Microwave Propagation", ICCCE, Kuala Lumpur, Malaysia, pp. 1156-1161, 2010.

[26]   C. C. Ku and H. Y. Chen, "Calculation of wave attenuation in sand and dust storms by the FDTD and turning bands methods at 10–100 GHz", vol. 36, pp. 2951-2960, 2012.

[27]   S. I. Ghobrial and S.M.Sharief, "Microwave attenuation and cross polarization in dust storms", vol. 35, pp. 418-427, 1987.

[28]   X. Jingming Y. Wenyan, "Cross polarization effect of circularly polarized microwave, millimeter wave propagation in the air suspending dust particles", vol. 5, pp. 44-50, 1990.

[29]   A. S. Ahmed, "Role of particle-size distributions on millimeter-wave propagation in sand/duststorms", vol. 134, pp. 55-59, 1987.

[30]   S. O. Bashir N. J. McEwan, "Microwave propagation in sand and dust storms: The theoretical basis of particle aligment", ICAP 1983, Norwich, pp. 40-44, 1983.

[31]   N.J.Mceman S.O.Bashir, "Crosspolarization and gain reduction due to sand or dust on microwave reflector antennas", vol. 21, pp. 379-380, 1985.

[32]   S. Haddad, S. A. Abdalla M. J. H. Salman, "Microwave attenuation and depolarization due to non-spherical dust particles", in Proc. Jordan IEEE'85, Amman, Jordan, pp. 333-337, 1985.

[33]   H. JiYing X. YingXia, "Effect of sand and dust storms on Ka-band electromagnetic wave propagation along earth-space paths", vol. 18, pp. 328-331, 2003.

T.S CHU, "Effects of sand storms on microwave propagation", pp. 549-555, 1979.

[34]   Y. Auchterlonie, L.Y. Ahmed, "Microwave measurements on dust using an open resonator", vol.12, pp. 445-446, 1976.

[35]   H. JiYing X. YingXia, "Effect of sand and dust storms on Ka-band electromagnetic wave propagation along earth-space paths", vol. 18, pp. 328-331, 2003.

[36]   S.I GHOBRIAL, "Effect of hydroscopic water on dielectric constant of dust at X-band", vol.16, p. 393—394, 1980.

[37]   H. T. Gupta, S.C. Al Mashadani, M Buni, K Al Hafid, "Study of microwave propagation under adverse dust storm conditions", 3rd World Telecom Forum, Geneva, 1979.

[38]   B. G. Holt, A.R. Evans, "A review of theoretical prediction techniques of transmission parameters for slant path earth-space communications", AGARD Conf, London, 1980.

[39]   B. G. Evans A.J Ansari, "Microwave propagation in sand and dust storms", vol. 129, 1982.

[40]   J. Goldhirsh, "Attenuation and backscatter from a derived two-dimensional duststorm model", vol. 49, pp. 1703-1711, 2001.

[41]   M. R. Islam, K. Al-Khateeb, A. Z. Alam, Z. O.Elshaikh E. A. A. Elsheikh, "A proposed vertical path adjustment factor for dust storm attenuation prediction", 4th International Conference On Mechatronics (ICOM), Kuala Lumpur, Malaysia, 2011.

[42]   J. Goldhirsh, "A parameter review and assessment of attenuation and backscatter properties associated with dust storms over desert regions in the frequency range of 1 to 10 GHz", vol. 30, pp. 1121-1127, 1982.

[43]   J. A. Jervase S. I. Ghobrial, "Microwave propagation in dust storms at 10.5 GHz-A case study in khartoum, sudan", vol. E-80 B, pp. 1722-1727, 1997.

[44]   M. R. Islam, A. H. M. Z. Alam, A. F. Ismail, K. Al-Khateeb, Z. Elabdin, E. A. A. Elsheikh, "The Effect of Particle Size Distributions on Dust Storm Attenuation Prediction for Microwave Propagation", International Conference on Computer and Communication Engineering (ICCCE 2010), Kuala Lumpur, Malaysia, May 2010.

[45]   M. R. Islam, O. O. Khalifa, H. E. Abd-El-Raouf Z. E. O. Elshaikh, "Mathematical model for the prediction of microwave signal attenuation due to duststorm", vol. 6, pp. 139-153, 2009.

[46]   S. Sharif J. Jervase, "Influence of duststorms and reflector tolerance on cross polarization of earth satellite links", Proc. Arabsat Symp, Riyadh, Saudi, 1988.

[47]   L. Gozalez, R. Codello J.Besse, "On The Performance Of Small Aperture Ka-Band Terminals For Use Over The Wideband Gapfiller Satellite", vol. 2, pp. 1388 – 1391, 2002.

[48]   Gary Comparetto, "The Impact of Dust and Foliage on Signal Attenuation in the Millimeter Wave Regime", vol. 11, pp. 13-20, 1993.

[49]   T K. Bandopadhyava & Saxena Poonam Khan Aftaal, "Effect Of Soil Textural Class And Relative Humidity Of Regions In Accurate Prediction Of Attenuation Of Millimeter Waves During Sand And Dust Storms", MSMW'2001 Symposium Proceedings. Kharkov, Ukraine, June 4 -9, 2001.

[50]   I. Y. Ahmed and L. J. Auchterlonie, "Microwave measurements on dust using an open resonator", vol. 12, p. 455, 1976.

[51]   S. I. Ghobrial, "Effects of hygroscopic water on dielectric constant of dust at X-band", vol. 16, pp. 393-394, 1980.

[52]   S. M. Sharief and S. I. Ghobrial, "X-band measurements of the dielectric constant of dust", Proc. Ursi Commission F 1983 Symposium, Louvain, Belgium, pp. 143-147, June 1983.

[53]   Gary Comparetto, "The Impact of Dust and Foliage on Signal Attenuation in the Millimeter Wave Regime," , vol. 11, pp. 13-20, 1993.

[54]   Julius Goldhirsh, "Attenuation and Backscatter From a Derived Two-Dimensional Duststorm Model", IEEE Transactions on Antennas and Propagation, vol. 49, no. 12, Dec. 2001.

[55]   Abbas Ali Lotfi-Neyestanak, Babak Mirzapour and Mohammad Jahan bakht, "Modeling the Local Rainfall Effects on Millimeter-Wave Propagation Using Homogeneous Meteorological Areas", IEEE Geoscience And Remote Sensing Letters, vol. 8, no. 6, November 2011.

[56]   D. V. Rogers and R. K. Crane, "Review of propagation results from the Advanced Communications Technology Satellite (ACTS) and related studies", *IEICE Trans. Commun.,* vol. E84-B, no. 9, pp. 2357–2368, Sep. 2001.

[57]   R. K. Crane, Propagation Handbook for Wireless Communication System Design. Boca Raton, FL: CRC Press, 2003.

[58]   R. K. Crane, "A local model for the prediction of rain-rate statistics for rain-attenuation models", IEEE Trans. Antennas Propagation, vol. 51, no. 9, pp. 2260–2273, Sep. 2003.

[59]   K. S. Chen and C. Y. Chu, "A propagation study of the 28 GHz LMDS system performance with M-QAM modulations under rain fading", Proc. Electromagnetic Res., PIER 68, vol. 68, pp. 35–51, 2007.

[60]   M. S. J. Singh, S. I. S. Hassan, M. F. Ain, F. Ghani, K. Igarashi, K. Tanaka, and M. Iida, "Rain attenuation model for South East Asia countries", Electron. Letters, vol. 43, no. 2, pp. 75–77, Jan. 2007.

[61]   J. S. Mandeep, S. I. S. Hassan, and K. Tanaka, "Rainfall measurements at Ku-band satellite link in Penang, Malaysia", IET Microwave, Antennas Propagation, vol. 2, no. 2, pp. 147–151, Mar. 2008.

[62] V. Ramachandran and V. Kumar, "Modified rain attenuation model for tropical regions for Ku-band signals", Int. J. Satellite Communication Network, vol. 25, no. 1, pp. 53–67, Jan./Feb. 2007.

[63] L. D. Emiliani, "Worst-month rain rate and rain attenuation statistics for satellite system sesign in a mountainous region in Colombia", IEEE Antennas Wireless Propagation Lett., vol. 5, no. 1, pp. 475–478, Dec. 2006.

[64] K. P. Liolis, A. D. Panagopoulos, and S. Scalise, "On the combination of tropospheric and local environment propagation effects for mobile satellite systems above 10 GHz", IEEE Trans. Veh. Technol., vol. 59, no. 3, pp. 1109–1120, Mar. 2010.

[65] V. Chandrasekar, H. Fukatsu, and K. Mubarak, "Global mapping of attenuation at Ku- and Ka-band", IEEE Trans. Geosci. Remote Sens., vol. 41, no. 10, pp. 2166–2176, Oct. 2003.

[66] Melnikov, Yeary, M.Huck and R. Kelley, "Potentials of frequency agile Ka and W band cloud radars", IEEE Radar Conference (RADAR), 2011, pp. 415-419, 2011.

[67] J. Jena and P. K. Sahu, "Rain fade and Ka-band Spot Beam Satellite communication in India", Recent Advances in Space Technology Services and Climate Change (RSTSCC) , pp. 304-306, 2010.

[68] Kamal Harb, Butt Omair, Samir Abdul-Jauwad, Abdullah Al-Yami, and AbdulAziz Al-Yami, "A Proposed Method for Dust and Sand Storms Effect on on Satellite Communication Networks" Innovations on Communication Theory (INCT), Istanbul, 2012.

[69] A. A. A. Abobakr S. Ahmed and M. A. Alhaider, "Measurement of atmospheric particle size distribution during sand/duststorm in riyadh, saudi arabia," Atmospheric Environment, vol. 21, no. 12, pp. 193–196, 1987.

[70] "A Brief Overview of Civilian Satellite Communciations in Australia", May 2009.

[71] "Effects of Sandstorms and Explosion-Generated Atmospheric Dust on Radio

Propagation," R. P. Rafuse, Technical Report Number DCA-16, Massachusetts Institute

of Technology Lincoln Laboratory, 10 November 1981.

[72] Currie, N. C., F. B. Dyer, and E. E. Martin, October 1976, "Millimeter Foliage

Penetration Measurements," Abstracts of the IEEE AP-Society Symposium, pp. 575-

577.

[73] Currie, N. C., E. E. Martin, and F. B. Dyer, December 1975, "Radar Foliage

Penetration

at Millimeter Wavelengths," Technical Report No. 4, Contract DAAA 25-73-C-0256,

Engineering Experiment Station, Georgia Institute of Technology.

[74] Currie, N. C., and C. E. Brown, 1987, Principles and Applications of Millimeter-

Wave

Radar, Artech House, Norwood, Massachusetts.

[75] Rafiqul MD Islam, Yusuf A Abdulrahman and Tharek A Rahman, *EURASIP

Journal on Wireless Communications and Networking* 2012, "An improved ITU-R rain

Attenuation prediction model over terrestrial microwave links in tropical region".

VITAE

NAME: Abdulaziz Mohammed AlYami

NATIONALITY: Saudi

DATE OF BIRTH: 15-01-1986

EMAIL: abdulaziz.yami.1@aramco.com

EDUCATION: B.S. in Electrical Engineering